

Metabolic glycoengineering – exploring glycosylation with bioorthogonal chemistry

Markus Kufleitner,  † Lisa Maria Haiber  † and Valentin Wittmann  *

Glycans are involved in numerous biological recognition events. Being secondary gene products, their labeling by genetic methods – comparable to GFP labeling of proteins – is not possible. To overcome this limitation, metabolic glycoengineering (MGE, also known as metabolic oligosaccharide engineering, MOE) has been developed. In this approach, cells or organisms are treated with synthetic carbohydrate derivatives that are modified with a chemical reporter group. In the cytosol, the compounds are metabolized and incorporated into newly synthesized glycoconjugates. Subsequently, the reporter groups can be further derivatized in a bioorthogonal ligation reaction. In this way, glycans can be visualized or isolated. Furthermore, diverse targeting strategies have been developed to direct drugs, nanoparticles, or whole cells to a desired location. This review summarizes research in the field of MGE carried out in recent years. After an introduction to the bioorthogonal ligation reactions that have been used in connection with MGE, an overview on carbohydrate derivatives for MGE is given. The last part of the review focuses on the many applications of MGE starting from mammalian cells to experiments with animals and other organisms.

1. Introduction

Glycosylation is a ubiquitous form of posttranslational modification,¹ and it has been estimated that a major proportion of all proteins is glycosylated.^{2,3} Besides glycoproteins, also glycolipids constitute an important class of glycoconjugates. The glycans within these conjugates are involved in numerous

cellular recognition and regulation processes.¹ Cell membrane-anchored glycoproteins, for example, are indispensable for cell–cell interaction, cell adhesion, proliferation, and differentiation. Moreover, carbohydrate structures can be the target for pathogens and toxins, and are involved in SARS-CoV-2 infection.⁴ Intracellular glycoproteins are found in all cell compartments, and the proteins belong to nearly all functional classes. Their functions reach from regulating protein activity, controlling protein localization to influencing interactions with other proteins or cellular pathways. Alterations in glycan structures are decisive to various aspects of cancer cell

Department of Chemistry and Konstanz Research School Chemical Biology (KoRS-CB), University of Konstanz, Universitätsstraße 10, 78457 Konstanz, Germany.

E-mail: mail@valentin-wittmann.de

† These authors contributed equally to this work.



Markus Kufleitner

Markus Kufleitner studied Life Science at the University of Konstanz (Germany). Within his Master studies, he stayed two semesters at the University of Toronto (Canada), working in Prof. Molly Shoichet's group. In 2018, he started his PhD within the Konstanz Fast Track program in the Wittmann group. Currently, he is working on the field of glycobiology and synthesizing next generation carbohydrate reporters.



Lisa Maria Haiber

Lisa Maria Haiber studied Life Science at the University of Konstanz (Germany). In 2018, she joined the Wittmann group as PhD student. Her project is focused on protein O-GlcNAcylation using metabolic glycoengineering as method of choice. Thereby, she uses the inverse electron demand Diels–Alder reaction for labeling proteins.

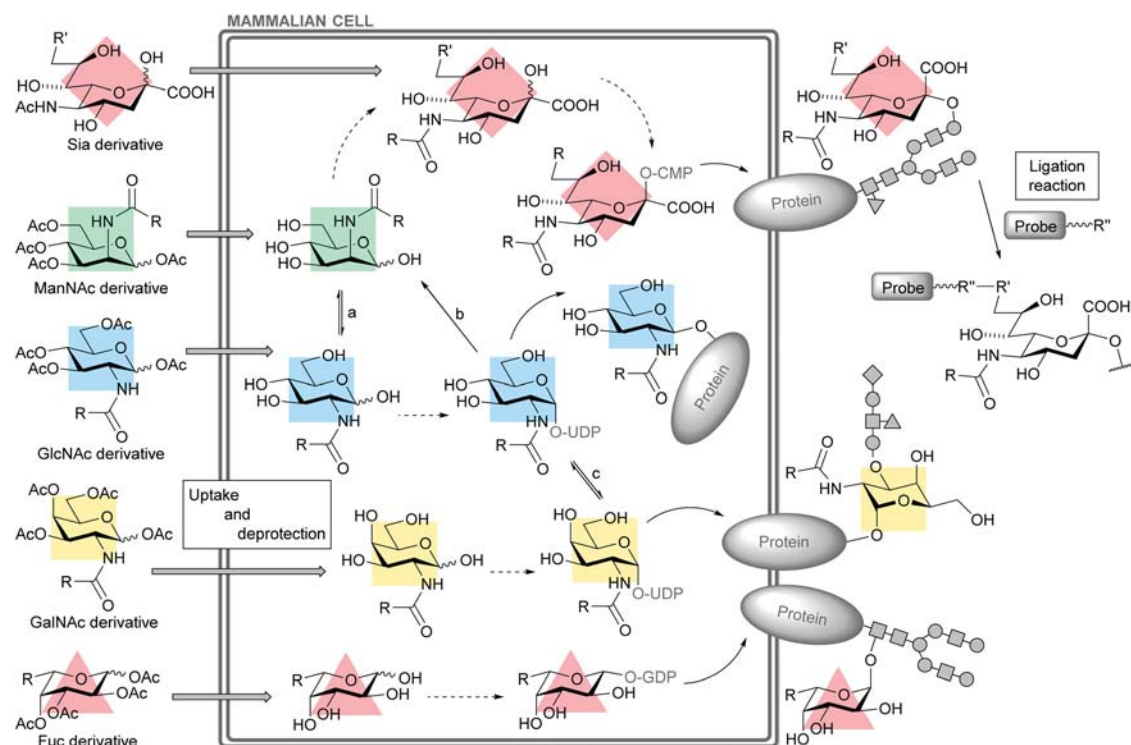


Fig. 1 Metabolic glycoengineering in mammalian cells with a simplified overview of the metabolic processes inside the cell resulting in incorporation of a sugar modified with a chemical reporter group (R, R') into glycan structures of glycoproteins. A subsequent bioorthogonal ligation reaction allows further derivatization of the engineered glycan. Enzymatic steps allowing the interconversion between different monosaccharides are marked: (a) GlcNAc 2-epimerase, (b) UDP-GlcNAc 2-epimerase, (c) UDP-galactose 4-epimerase (GALE).

behavior. Cell-surface carbohydrate patterns of glycoproteins and glycolipids are altered in degenerated cells making them suitable tumor markers and possible anchor points for diagnostic and therapeutic approaches. Genetic defects resulting in

aberrant glycosylation are often lethal or have major consequences for living organisms.

While tagging of proteins with green fluorescent protein (GFP) set a new benchmark for the visualization and analytics in protein research,⁵ a comparable genetic method is not available for carbohydrates, which are secondary gene products. Three decades ago, metabolic oligosaccharide engineering (MOE) or metabolic glycoengineering (MGE) as it will be referred to in this review⁶ has been developed as a method to overcome this limitation.^{7,8} When studying the biosynthesis pathway of sialic acids, Reutter and coworkers found that *N*-propanoyl-*D*-mannosamine is accepted by the cellular enzymatic machinery in rats, converted to *N*-propanoylneuraminic acid and incorporated into cell surface glycans.⁹ Subsequently, the Bertozzi group showed that not only aliphatic chain elongation is an accepted modification for *N*-acetyl-*D*-mannosamine (ManNAc), but also the introduction of functional groups.¹⁰ In this fashion, functionalized glycans appeared on the cell surface, where they could be labeled for detection. Today, MGE is an established and widely used method for the labeling of not only sialic acids but all sorts of glycan structures in cells and whole organisms including animals.^{11–15}

In this approach, synthetic sugar derivatives bearing a functional group with a unique chemical reactivity – a so-called chemical reporter group¹⁶ – are fed to cells or organisms upon which they enter the salvage pathway and subsequently are incorporated into the glycan structures by the biosynthetic



Valentin Wittmann

Valentin Wittmann obtained a PhD from the Technical University of Munich (Germany). Subsequently, he carried out post-doctoral research at the Goethe-University of Frankfurt (Germany) and at The Scripps Research Institute in La Jolla, California (USA). In 1997 he returned to Frankfurt to start independent research. Since 2003 he is professor of organic/bioorganic chemistry at the University of Konstanz (Germany). From 2006

until 2011 he was Dean of Studies, from 2016 until 2020 head of the Department of Chemistry, and since 2016 he is vice coordinator of the Collaborative Research Center SFB 969. His main research area is the chemical biology of carbohydrates including metabolic glyco-engineering, investigation of multivalent carbohydrate-protein interactions, and RNA-targeting antibiotics.

machinery of the cells (Fig. 1). Typically, peracetylated saccharides are used in order to pass the cell membrane by passive diffusion making the delivery of these compounds straightforward.¹⁷ Once inside the cell, the sugars are deprotected by nonspecific esterases and further metabolized to end up as “unnatural” sugar moieties on glycosylated structures. Bioorthogonal ligation chemistry allows further derivatization with various probes for visualization, profiling, enrichment, or targeting the glycoconjugates. Depending on the incorporated chemical reporter group, different chemistries can be employed for bioorthogonal ligation.

For the application of MGE, it is fundamental to understand the acceptance of the unnatural sugars by the involved enzymes and the biosynthetic pathways of glycans. The fact, that natural sugars and often also modified ones are converted into each other by epimerases, makes the situation complex. In the following, we describe the main metabolic pathways that are crucial for MGE experiments (Fig. 1). Cell surface *N*- and *O*-glycans as well as glycolipids can be heavily sialylated at the non-reducing end of the glycan structures. ManNAc is the main precursor for *N*-acetyl neuraminic acid (Neu5Ac), an abundant representative of sialic acids. The metabolic pathway towards an unnatural CMP-sialic acid, the activated nucleotide sugar used by transferases, can be shortened when a modified sialic acid derivative is directly used as a sugar reporter. However, ManNAc derivatives are synthetically easier accessible than sialic acid derivatives and, therefore, often the preferred precursors.

N-Acetyl-*D*-glucosamine (GlcNAc) derivatives can enter the GlcNAc salvage pathway and are converted in three enzymatic steps to the corresponding UDP-GlcNAc derivatives, which are the substrate for *O*-GlcNAc-transferase (OGT) and other glycosyltransferases. OGT modifies proteins in the cytosol, nucleus, and other cell compartments with a single GlcNAc residue (*O*-GlcNAcylation). Furthermore, UDP-GlcNAc can be converted to ManNAc by UDP-GlcNAc 2-epimerase enabling GlcNAc derivatives to enter the metabolic pathway for sialic acids. Moreover, also GlcNAc can be reversibly converted to ManNAc by GlcNAc 2-epimerase.^{18,19}

UDP-GalNAc is synthesized in two enzymatic steps from *N*-acetyl-*D*-galactosamine (GalNAc) in the GalNAc salvage pathway. *N*-Acetylgalactosamine-transferases (GalNAc-Ts) use UDP-GalNAc as activated nucleotide sugar to synthesize *O*-GalNAc glycans that are further converted to mucin-type *O*-glycans. UDP-GalNAc can be epimerized to UDP-GlcNAc by UDP-galactose 4-epimerase (GALE). This allows GalNAc derivatives to be used as *O*-GlcNAc reporters²⁰ and potentially be even converted to sialic acid derivatives. Finally, *L*-fucose (Fuc) and derivatives thereof can be converted to GDP-Fuc, the corresponding nucleotide sugar, which is the substrate for fucosyltransferases.

With this toolbox in hand, numerous applications of MGE are possible reaching from labeling cell surfaces in cell culture to the tracing and profiling of glycans in organisms and the development of diverse targeting strategies. The application of MGE in combination with a subsequent bioorthogonal ligation reaction to label glycans is advantageous over the use of lectins or antibodies with low binding affinity or cross-reactivity

because the reporter group is directly embedded in the glycans and reacts with high selectivity in the labeling reaction.¹¹ Furthermore, the unnatural sugar derivative can be added at different points of time allowing to detect changes of glycosylation levels *e.g.* in response to a signal. A limitation of MGE is the altered acceptance of the unnatural sugars by the processing enzymes, which can result in low incorporation efficiencies or altered interconversion by epimerases. Another limitation of MGE is the perturbation of the cellular system by feeding unnatural carbohydrates, which might result in different glycosylation levels and lowered recognition of glycans by their binding partners.

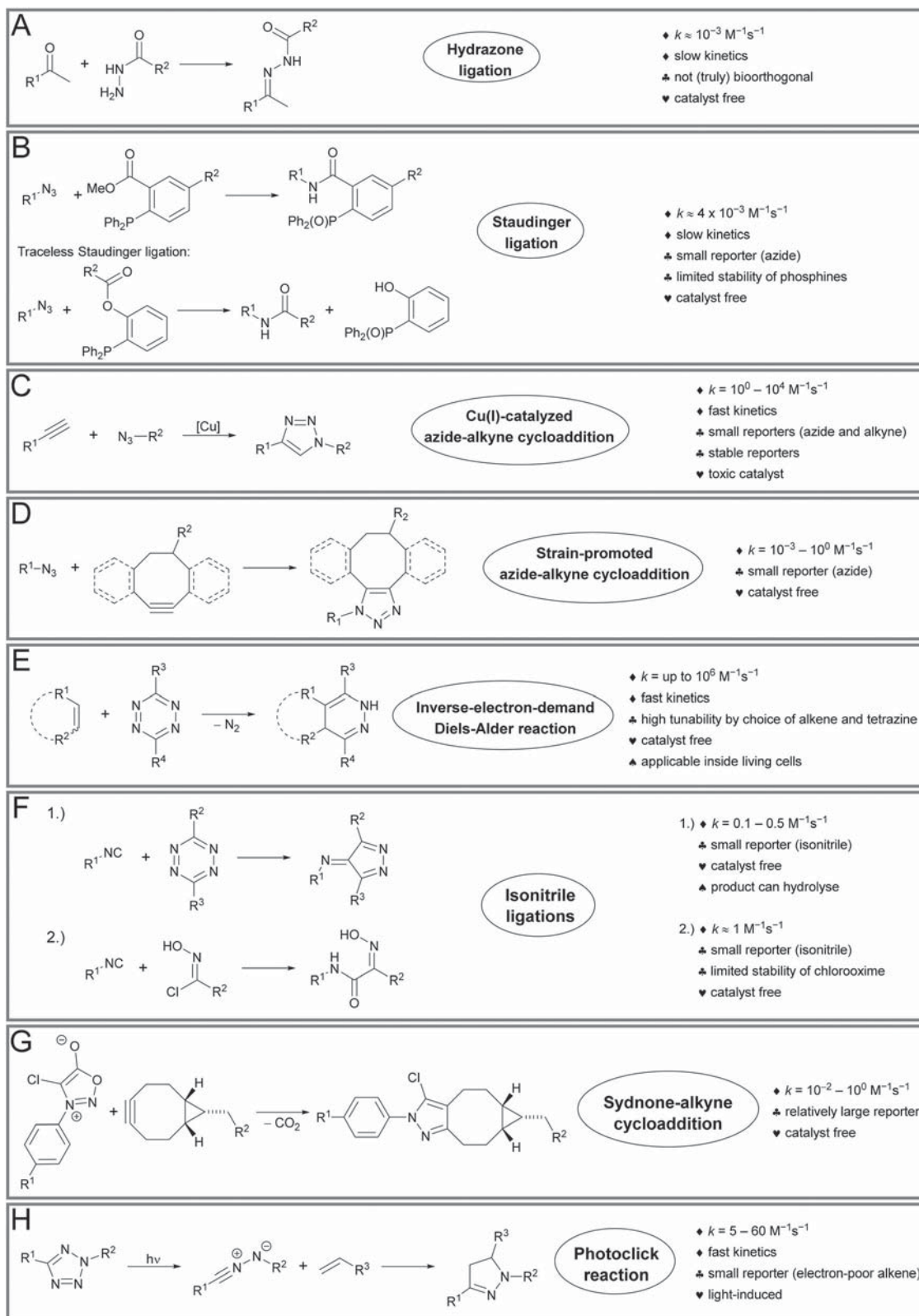
In this review, we focus on the developments of the last 10 years. The ligation reactions that have been used in MGE will be introduced in Chapter 2. An overview of carbohydrates that are derivatized with a chemical reporter group and that have been used in MGE, is given in Chapter 3. Chapter 4 then summarizes applications of MGE starting from cell culture and reaching to experiments in higher organisms. This article focuses on the application of MGE in mammalian cells, tissue, and animals. Other higher eukaryotic organisms including zebrafish and plants are briefly discussed. MGE has also been applied to bacteria as summarized in recent review articles.^{21–23} These studies are not included here.

2. Bioorthogonal ligation reactions for MGE

Bioorthogonal reactions are defined as chemoselective reactions that are so selective that they can be carried out even in living cells or organisms without interaction or interference with the biological system.^{16,24,25} The term bioorthogonal chemistry was introduced by Bertozzi in 2003²⁶ although the general concept is much older with strong roots in the field of bioconjugation. It is questionable whether “truly” bioorthogonal reactions exist at all because it will probably not be possible to exclude *any* interaction or interference with the biological system. However, the degree of bioorthogonality of many reactions is impressive and the concept has strongly advanced the field of chemical biology and stimulated the way how chemists think about chemical reactions. In 2022, Bertozzi, Meldal, and Sharpless were honored with the Nobel prize in chemistry “for the development of click chemistry and bioorthogonal chemistry”.²⁷ In this chapter, we focus on bioorthogonal ligation reactions that have been applied in MGE. For a more complete treatment of this topic, the reader is referred to recent reviews on bioorthogonal chemistry.^{28–34}

2.1 Hydrazone ligation

The reaction of aldehydes and ketones with hydrazides leads to the formation of acylhydrazones (Fig. 2A).³⁵ In the very first report on metabolic glycoengineering using a chemical reporter group, ketone moieties were introduced into glycans by culturing cells with a ketone-modified ManNAc derivative, ManLev.¹⁰ Later, the peracetylated sugar Ac₄ManLev was employed.³⁶



◆ information about kinetics; ▲ information about reporter groups; ▼ information about necessary catalysts; ▲ additional information

Fig. 2 Ligation reactions used in combination with MGE.

Subsequently, hydrazone ligation was used to modify the ketone reporter groups with a hydrazide-biotin conjugate. Although not

truly bioorthogonal, the reaction was successfully utilized to modify ketone-containing glycans on the cell surface.

In general, hydrazone ligation tends to be incomplete and slow (second-order rate constant $k \approx 10^{-3} \text{ M}^{-1} \text{ s}^{-1}$)³⁷ with the possibility to increase the reaction speed by lowering the pH.³⁵ Furthermore the reaction is reversible questioning the stability of the formed conjugates. Nevertheless, the reaction found widespread application in other areas than MGE, for example for the preparation of carbohydrate and peptide conjugates, the immobilization of carbohydrates on chip surfaces and many more.³⁸ In MGE, hydrazone ligation has been largely replaced by ligation reactions with improved properties, such as the azide-alkyne cycloaddition or inverse-electron-demand Diels-Alder reaction, which will be described below.

2.2 Staudinger ligation

To overcome the limitations of the hydrazone ligation, Bertozzi and coworkers developed the Staudinger ligation as a truly bioorthogonal reaction.¹⁷ In the classical Staudinger reduction reported in 1919, an azide is reduced by a phosphine, such as triphenyl phosphine, to yield an amine.³⁹ As an intermediate, a nucleophilic azaylide (also termed iminophosphorane) is formed under release of nitrogen. By introducing an electrophilic trap (*e.g.*, a methyl ester) to the phosphine, this nucleophilic intermediate can be trapped to form a stable amide bond (Fig. 2B).^{17,40} In contrast to aldehydes and ketones required for hydrazone ligation, azides are not yet found to occur in biological systems.⁴¹ Azides are weak electrophiles that are inert to nucleophilic attack. In combination with their small size that causes only minimal changes in a molecule, these properties make azides frequently used reporter groups that cannot only be used for Staudinger ligation but also for azide-alkyne cycloadditions (*vide infra*).

The Staudinger ligation was the first example of a bioorthogonal ligation reaction, which can be performed not only in cell culture, but also in living animals, allowing new possibilities for application.⁴² However, compared with newer ligation reactions, the Staudinger ligation is rather slow ($k \approx 4 \times 10^{-3} \text{ M}^{-1} \text{ s}^{-1}$).⁴⁰ A traceless version of the reaction has been also reported.^{43,44} In this variant, the phosphine oxide residue is cleaved off during the hydrolysis step.

2.3 Copper-catalyzed azide-alkyne cycloaddition

The copper catalyzed azide-alkyne [3+2] cycloaddition (CuAAC) leading to the formation of 1,4-disubstituted triazoles (Fig. 2C) is one of the most prominent bioorthogonal ligation reactions as it is fast, reliable, and high yielding. Terminal alkynes and azides are convenient functionalities to react in a biological environment. Alkynes appear in biological systems only rarely^{45,46} and do not tend to interact with the functional groups occurring inside cells. As an improvement of the original Huisgen azide-alkyne cycloaddition,^{47,48} the copper(I)-catalyzed version was independently published in 2002 by Meldal⁴⁹ and Fokin and Sharpless.⁵⁰ With a second order rate constant k of 10^0 – $10^4 \text{ M}^{-1} \text{ s}^{-1}$,³⁴ it is orders of magnitude faster than the uncatalyzed reaction. The reaction proceeds *via* a binuclear copper acetylide intermediate as determined by heat-flow reaction calorimetry and crossover



Fig. 3 Copper(I) ligands frequently used for CuAAC.

experiments with differently isotopically enriched copper complexes.⁵¹

Experimentally, the copper(I) species can be either used directly or be generated *in situ* by adding copper(II) salts and a reducing agent, for example sodium ascorbate or tris(2-carboxyethyl)phosphine (TCEP).⁵⁰ The addition of copper(I) ligands, such as the ones depicted in Fig. 3, improves the reaction by maintaining the oxidative state of the copper species and protection of biomolecules from oxidative harm during the bioorthogonal reaction.^{52,53} Numerous copper(I) ligands including water-soluble ones have been reported²⁸ although not all of them have been applied in MGE. CuAAC is broadly used for bioorthogonal labeling, however, it is limited in its application when it comes to living systems. Copper species can lead to oxidative stress inside cells and interact with cysteine thiols.⁵⁴ Although the above-mentioned copper ligands reduce these effects, they cannot fully overcome the toxicity problem. Nevertheless, labeling of the surface of living cells is possible as was shown after MGE with an azido mannosamine derivative.⁵⁵ CuAAC is not only popular in bioconjugate chemistry but in all areas of chemistry including drug discovery, proteomics, and material science.^{56,57}

2.4 Strain-promoted azide-alkyne cycloaddition

In 1961, Wittig and Krebs characterized the product of the quickly proceeding reaction between cyclooctyne and phenyl azide to be a triazole.⁵⁸ Based on this observation, the Bertozzi group established this strain-promoted azide-alkyne cycloaddition (SPAAC, Fig. 2D) as a bioorthogonal ligation reaction using an azido modified sugar derivative.⁵⁹ Cyclooctyne, which is the smallest cycloalkyne that can be isolated and stored without decomposition, has bond angles of the sp-hybridized carbons of 153° and 155° leading to a significant amount of ring strain.⁶⁰ These bond angles are closer to the transition state geometry of the Huisgen azide-alkyne cycloaddition than those of an acyclic terminal alkyne. Accordingly, the increased reactivity of cyclooctynes with azides can be explained by the lower energy required to distort the alkyne into the transition-state geometry.⁶⁰

Although SPAAC of cyclooctyne proceeds much faster than the original Huisgen 1,3-dipolar cycloaddition, the reaction is still relatively slow. After the seminal paper by Bertozzi,⁵⁹ several attempts have been undertaken to accelerate the reaction rate of this reaction which is nowadays often referred to as

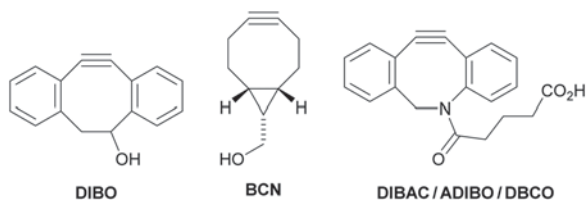


Fig. 4 Cyclooctynes commonly used in SPAAC.

“copper-free click reaction”. For example, fluorine substituents adjacent to the alkyne functionality^{61–63} increase the interaction energy and thereby the reaction rate.⁶⁰ (Di)benzoannulation is another means to accelerate the reaction. The effect has been explained by the increased ring strain due to the presence of several sp^2 -hybridized carbon atoms resulting in a decreased distortion energy.⁶⁴ However, more recent studies employing distortion/interaction analysis explain the increased reaction rate by a greater interaction energy.⁶⁵ For a detailed analysis of the mechanism of SPAAC and other metal-free bioorthogonal ligation reactions see the recent review article from Franzini.²⁹ Further examples of cyclooctyne derivatives for SPAAC have been developed.^{29,66} Today, the cyclooctynes most commonly used in SPAAC are DIBO, BCN, and DIBAC (also known as ADIBO or DBCO, the latter of which is now the most commonly used abbreviation) (Fig. 4), which represent a good compromise between reactivity and stability. Furthermore, they are commercially available. While cyclooctynes are inert against amines and hydroxy groups, they react with thiols⁶⁷ which limits application of SPAAC inside living cells. Although originally developed for MGE,⁵⁹ SPAAC is now part and parcel of the toolkit of bioorthogonal ligation and used in numerous applications.⁶⁶

2.5 Inverse-electron-demand Diels–Alder reaction

The inverse electron demand Diels–Alder (IEDDA) reaction of 1,2,4,5-tetrazines, acting as electron-poor dienes, with electron-rich dienophiles (Fig. 2E) was initially reported in 1959.⁶⁸ In 2008, the reaction was applied by three research groups for the first time in the field of bioconjugation. The Fox group used *trans*-cyclooctene (TCO) as dienophile,⁶⁹ the Hilderbrand group used norbornene,⁷⁰ and the Braun group a tetracyclic dienophile containing a cyclobutene and a second strained alkene⁷¹ allowing even a sequential ligation reaction. Since then, the IEDDA reaction has developed to one of the most often applied ligation reactions. Among the reasons for its popularity are the fast reaction kinetics, especially when carried out in water, with second-order rate constants up to $10^6 \text{ M}^{-1} \text{ s}^{-1}$ without the need for metal catalysts, its bioorthogonality, and the fact that the reaction is irreversible (in contrast to the normal-electron-demand Diels–Alder reaction). The IEDDA ligation proceeds in two steps, a cycloaddition to a bicyclic intermediate followed by a retro-Diels–Alder reaction accompanied by nitrogen gas release (accounting for the irreversibility). The formed dihydropyridazines can exist in several tautomeric forms and are often further oxidized to the aromatic pyridazines by either oxygen or excess of tetrazine.

Dienophiles span an enormous range of reactivity for the IEDDA reaction with tetrazines. Whereas TCO derivatives are the fastest reaction partners for tetrazines known, two aspects limit their suitability for MGE. TCOs have a limited stability and can isomerize to *cis*-cyclooctynes that have a reactivity many orders of magnitude below that of TCOs. In addition, TCOs are sterically demanding groups limiting their application as reporter groups in metabolic labeling. Accordingly, the first application of the IEDDA reaction in combination with MGE made use of 1-methylcyclopropenes.⁷² The methyl substituent at the double bond increases the stability of cyclopropene towards nucleophilic attack and polymerization. Later on, however, also derivatives without a methyl substituent that are stable enough to survive the conditions during MGE have been developed.^{73,74} Depending on the type of attachment of the cyclopropene moiety, its reactivity with tetrazines can vary significantly. For example, a carbamate-modified methylcyclopropene was shown to react 100 times faster than an amide-modified derivative.⁷⁵ Terminal alkenes represent alternative dienophiles for the IEDDA reaction with tetrazines. Their reactivity is even lower than that of cyclopropenes ($k \approx 10^{-3}$ – $10^{-1} \text{ M}^{-1} \text{ s}^{-1}$) but they do not suffer from any instability issues making them a label of choice when reaction speed is not a limiting issue. More recently, even large reporters, such as norbornenes⁷⁶ and TCO⁷⁷ have been employed for MGE. A major advantage of the IEDDA reaction over CuAAC and SPAAC is its suitability for applications inside living cells. In the field of MGE, this has been demonstrated for studying protein-specific O-GlcNAcylation of EGFP-labeled proteins by FLIM-FRET microscopy.⁷⁸

2.6 Isonitrile-tetrazine and isonitrile–chlorooxime ligation

Isonitriles are promising reporter groups due to their small size and compatibility with biological systems. They can participate in two different bioorthogonal ligation reactions (Fig. 2F). With tetrazines, they react in a [4+1] cycloaddition to form – *via* unstable tetraazanorbornadienimines – under nitrogen release 4*H*-pyrazol-4-imine derivatives. Tertiary isonitriles react faster ($k \approx 0.6 \text{ M}^{-1} \text{ s}^{-1}$) than primary isonitriles ($k \approx 0.1 \text{ M}^{-1} \text{ s}^{-1}$) and form products that are quite stable in aqueous systems with a half-life of several days.⁷⁹ Hexosamine derivatives with tertiary isonitriles as reporter groups showed only limited success in MGE so far, possibly due to their large size.⁸⁰ MGE employing hexosamine derivatives with primary isonitriles on the other hand resulted in much higher signal-to-background ratio after cell-surface labeling. However, it is crucial to design the isonitrile in a way that the cycloaddition product with the tetrazine is stabilized and does not quickly hydrolyze.^{79,80} Currently the isonitrile–tetrazine reaction is more often used for click-to-release strategies than as a ligation reaction.⁸¹

Recently, a second bioorthogonal ligation reaction with isonitriles as reporter group, the isonitrile–chlorooxime ligation, was reported by the Wennemers group.⁸² Here, the chlorooxime releases hydrogen chloride in aqueous solution and forms a nitrile oxide, which can be attacked by the isonitrile. The formed nitrilium ion can further react with water to form an α -hydroxyimino amide. The rate constant of the

reaction was determined to be $k \approx 1 \text{ M}^{-1} \text{ s}^{-1}$. In a cellular context, a ManNAc derivative with an isonitrile reporter group was used to visualize cell surface glycosylation after labeling with the isonitrile–chlorooxime ligation. The limited stability of the chlorooxime prevents its use as a reporter group. A limitation of the isonitrile–chlorooxime ligation is the interference of thiols. This issue can be addressed by performing the reaction at pH 5.5, conditions which are not met inside living cells. Therefore, the reaction is not suitable for intracellular applications but can be applied on the cell surface.

2.7 Sydnone–alkyne cycloaddition

Another bioorthogonal [3+2] cycloaddition is the reaction of arylsydnones with alkynes (Fig. 2G). As the other [3+2] cycloadditions mentioned before, this reaction is also based on the early work of Huisgen.⁸³ In earlier studies, a copper-catalyzed version of this reaction with terminal alkynes has been reported.⁸⁴ Similar to SPAAC, it is possible to circumvent the need for copper-catalysis by utilizing ring-strained alkynes as driving force of the reaction.⁸⁵ For bioconjugation, mainly BCN is used as the ring-strained alkyne of choice. The reaction rate can be further accelerated by introducing halogen substituents, especially chloro substituents, at the 4 position of the sydnone resulting in second-order rate constants ($k \approx 10^{-2}$ – $10^0 \text{ M}^{-1} \text{ s}^{-1}$) comparable to those for SPAAC.^{86,87} Different fluorogenic sydnone probes have been reported for protein labeling.^{88,89} Moreover, the reaction has been used also for bioconjugation after MGE⁹⁰ and to label DNA postsynthetically.⁹¹

2.8 Photoclick reaction

In 2007, Lin and coworkers re-discovered the possibility to synthesize pyrazolines *via* a photoactivated 1,3-dipolar cycloaddition (Fig. 2H),⁹² which was already reported by Huisgen in 1967.⁹³ The first step is the photoinduced generation of a nitrile imine from a 2,5-diaryl-tetrazole, which proceeds fast with a first-order rate constant of $k_1 \approx 0.1 \text{ s}^{-1}$.⁹⁴ The following cycloaddition between the nitrile imine and a favorably electron-poor alkene leads to the formation of a fluorescent pyrazoline and is the rate determining step ($k_2 \approx 5$ – $60 \text{ M}^{-1} \text{ s}^{-1}$).⁹⁵

The effects of substituents at the tetrazole as well as the influence of the alkene on reaction kinetics, stability, conversion rate and irradiation wavelength were investigated by the Lin group leading to the successful labeling of proteins with genetically encoded alkene-functionalized amino acids.^{95–98} In 2019, the Wittmann group demonstrated the application of the photoclick reaction in MGE.⁹⁹ The reaction was further deployed in nucleic acid modification¹⁰⁰ and in material science^{101,102} For the application in bioorthogonal chemistry the photoclick reaction benefits from the lack of toxic metal catalysts, time and spatial monitoring and fast reaction kinetics.

3. Sugar derivatives for MGE

Fig. 5 depicts selected carbohydrate derivatives that have been used for MGE, which can enter the biosynthetic network shown

in Fig. 1 at different points of entry. Most of these derivatives are peracetylated to facilitate cellular uptake by passive diffusion over the cell membrane. Some derivatives contain protected phosphate groups at the anomeric center to bypass potential bottlenecks within the biosynthetic pathways. The application of these sugar derivatives in various experiments is described in Chapter 4.

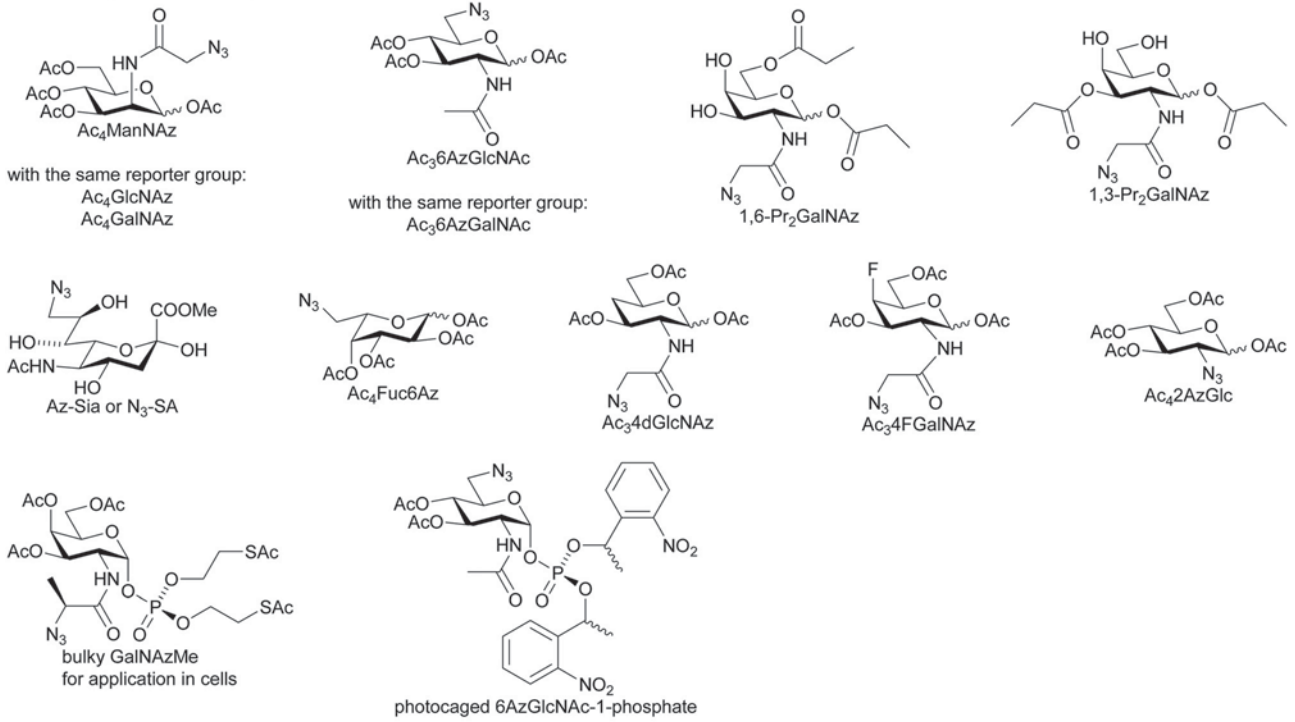
4. Application of MGE: from cells to organisms

4.1 Visualization of glycosylation in cell culture

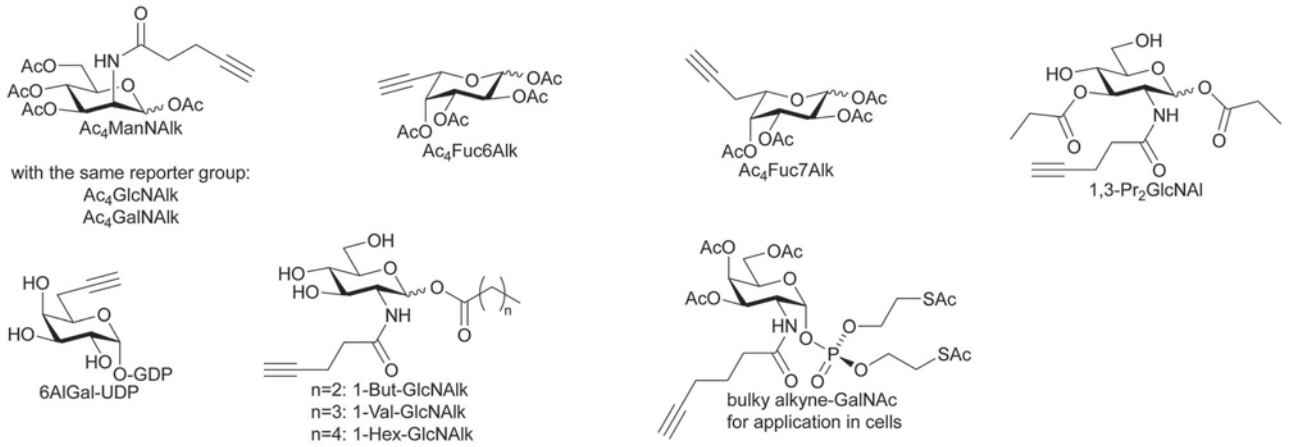
The first reports on MGE described the detection of cell surface glycosylation by flow cytometry making use of ketone- and azide-modified ManNAc derivatives, ManNLev and later Ac₄ManNAz, which are metabolized to and incorporated as sialic acids.^{10,17} The concurrent labeling with Ac₄ManNLev and Ac₄ManNAz combining hydrazone ligation and Staudinger ligation was reported soon after by the Bertozzi group.³⁶ In 2006, the Wong group reported the use of Ac₄Fuc6Az to visualize glycosylation by confocal fluorescence microscopy after labeling glycoconjugates of fixed cells with a dye by CuAAC.¹⁰³ The Bertozzi group imaged sialylated glycans after incubating cells with Ac₄ManNAz and labeling with a phosphine–dye conjugate by Staudinger ligation.¹⁰⁴ In the following, alkynyl-modified monosaccharides, Ac₄Fuc6Alk and Ac₄ManNAalk, were developed and used in combination with CuAAC to image fixed cells.¹⁰⁵ Another alkynyl-fucose, Ac₄Fuc7Alk, was reported later.¹⁰⁶ Elongation of the carbon chain between the reporter group and the sugar led to a more specific substrate for fucosyltransferase FUT8, which is responsible for core fucosylation of *N*-glycans. Visualization was achieved by a two-step labeling after CuAAC with biotin azide and a dye–streptavidin conjugate (Fig. 6A).

Since the selective incorporation of unnatural sugar reporters into the glycan structures of a single protein is inherently difficult, techniques were developed to allow protein-specific visualization of glycosylation. These approaches mainly rely on the introduction of a second probe targeting the protein of interest to achieve selectivity although all glycans are stained by MGE. Förster resonance energy transfer (FRET) based fluorescence microscopy of a GFP-tagged protein with labeled glycans was established and used to detect the effect of different glycoforms on the internalization behavior of GLUT4 glucose transporter.¹⁰⁷ A two-photon fluorescence lifetime imaging microscopy (FLIM) approach further addressed the protein-specific imaging.¹⁰⁸ Glycoproteins were labeled with Ac₄ManNAz, and a second fluorophore was introduced with a small, tagged antigen-binding fragment making this technique independent of the need for GFP-tagged proteins. Recently a similar approach was reported.¹⁰⁹ Here, fluorescently labeled aptamers in combination with MGE with Ac₄ManNAz enabled to study the glycosylation of specific exosomal proteins. Ac₄ManNAalk was used for protein-specific imaging of sialylated glycans with a method based on *cis*-membrane FRET.¹¹⁰ Using IEDDA chemistry, it is possible to visualize protein-specific

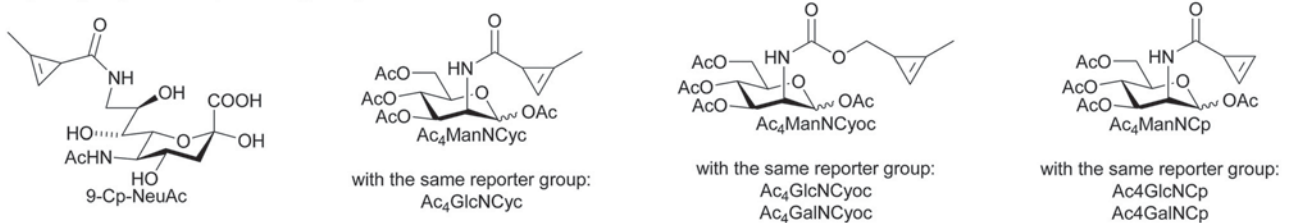
Azide reporter groups:



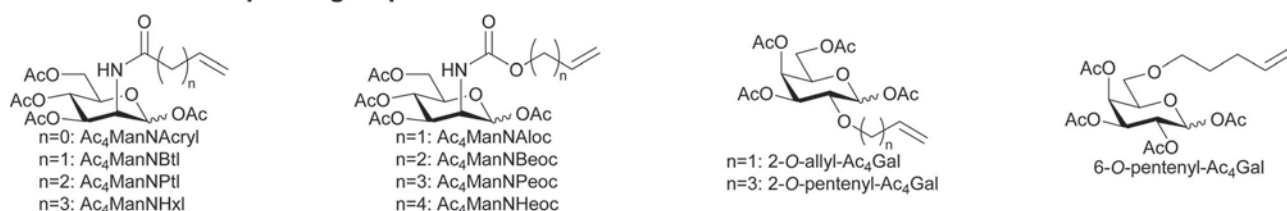
Terminal alkyne reporter groups:



Cyclopropene reporter groups:



Terminal Alkene reporter groups:



Miscellaneous reporter groups:

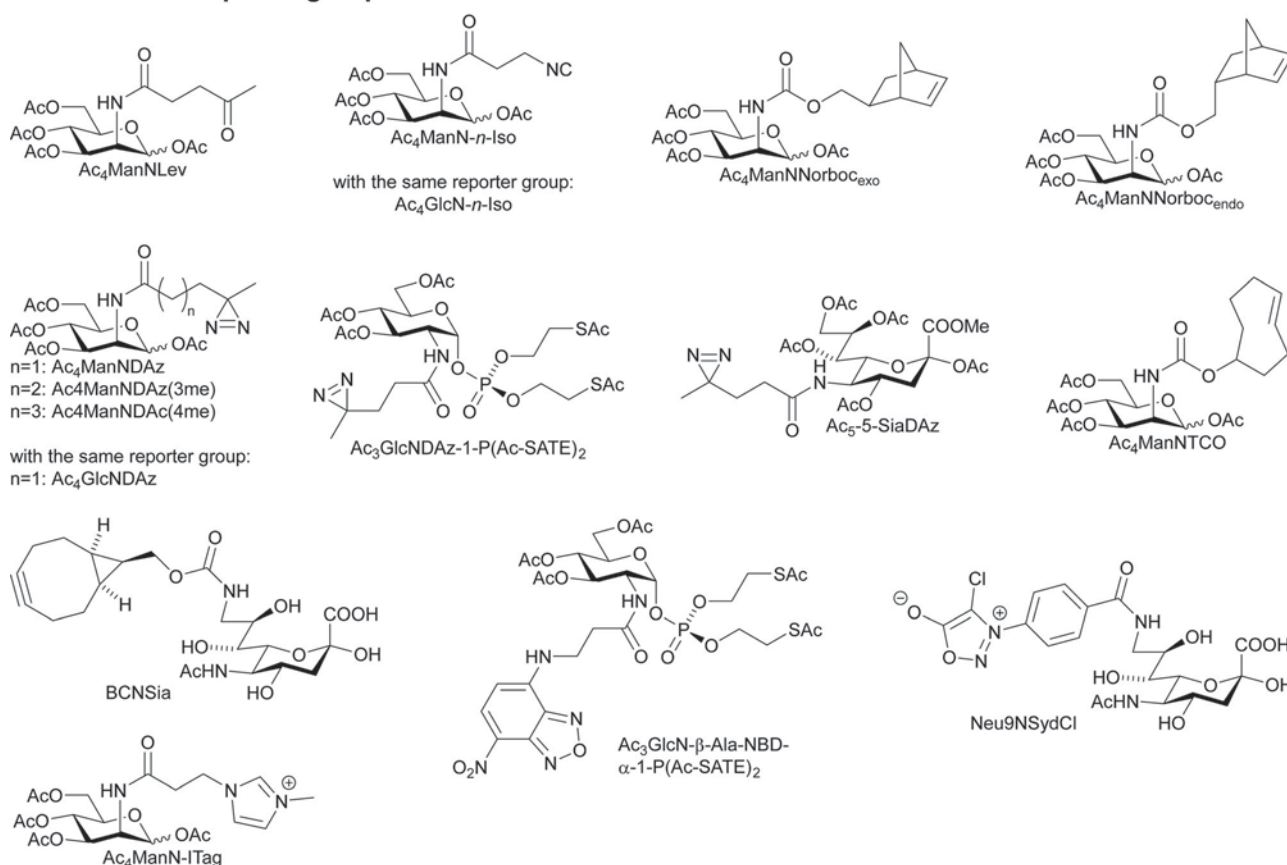


Fig. 5 Carbohydrate derivatives functionalized with a chemical reporter group for MGE.

labeling even within living cells.⁷⁸ Imaging of neighboring sugars was reported with an upconversion luminescent nanoparticle functionalized with an aptamer to allow targeting of specific proteins.¹¹¹ Another method was specifically designed to address receptor proteins.¹¹² In this approach, the donor fluorophore was fused to a receptor-specific ligand to bring it in proximity to the glycan structures of the protein.

Other techniques for signal creation or enhancement for imaging were adapted for MGE. DNA rolling circle amplification was used to detect cell surface glycosylation after incubating cells with azido sugars in low concentrations of 5 μ M.^{113,114} Proximity-induced hybridization chain reaction was shown to be suitable for visualizing protein-specific sialylation after incubating cells with Ac₄ManNAz and subsequent treatment with two DNA probes, one specific for the unnatural sugar and

one specific for the protein of interest.¹¹⁵ Another study combined hybridization chain reaction with FRET to visualize GalNAz on the cell surface.¹¹⁶

Starting in 2012, the IEDDA reaction emerged as a ligation reaction for MGE especially suitable for live cell imaging.³¹ A variety of reporter groups was presented, differing in their size and reaction kinetics in the IEDDA reaction. ManNAc derivatives modified with terminal alkenes were used to visualize cell surface sialylation with IEDDA chemistry.¹¹⁷ Simultaneous incubation of cells with pentenyl-modified Ac₄ManNPtl and Ac₄GalNAz followed by IEDDA and SPAAC labeling allowed the dual labeling of two different sugars after MGE (Fig. 6B and C). Alteration of the linkage of the alkene reporter group to the sugar from an amide bond to a carbamate resulted in another set of alkene-modified ManNAc derivatives suitable for cell

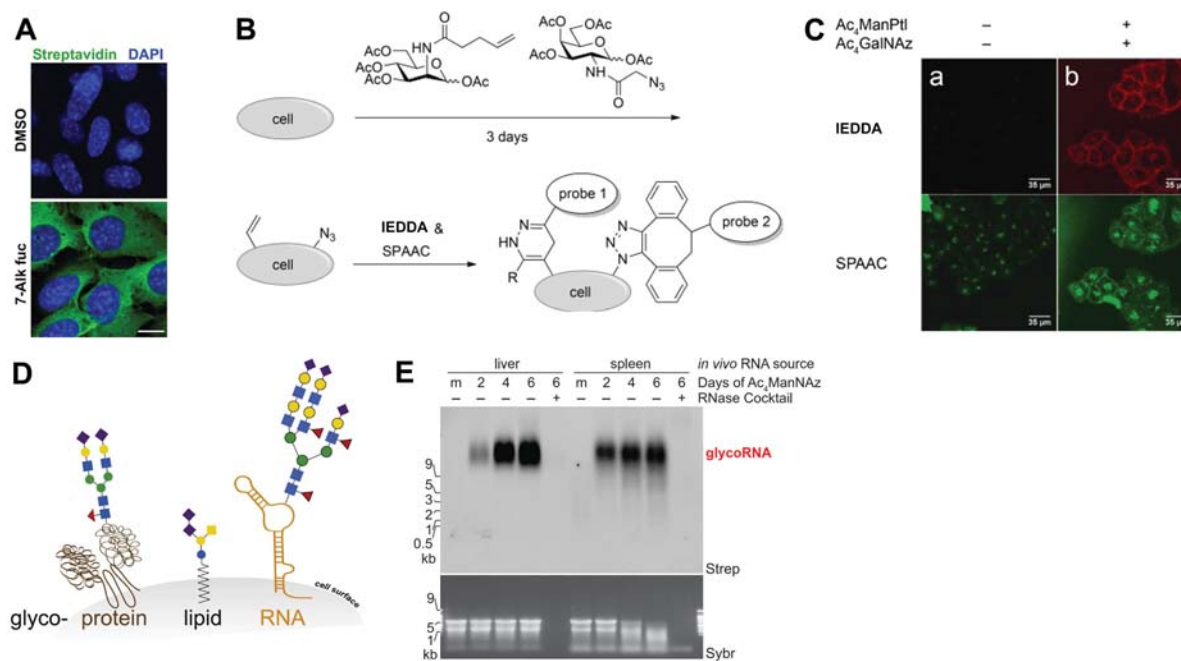


Fig. 6 (A) Fluorescence microscopy images of fixed MEF cells treated with Ac₄Fuc7Alk and labeled with an azide–biotin conjugate followed by streptavidin–AlexaFluor488 staining. Nuclei were counter stained with DAPI. Scale bar: 10 μm. Reproduced with the permission from ref. 106. Copyright 2016, Elsevier Ltd. (B) Schematic depiction of a dual-labeling strategy for MGE with alkene-modified Ac₄ManNPTl and azide-modified Ac₄GalNAz and subsequent labeling with two orthogonal ligation reactions. Reproduced with the permission from ref. 117. Copyright 2013, Wiley-VCH Verlag GmbH & Co. KGaA. (C) Fluorescence microscopy image of live HeLa cells after dual labeling with two different sugars and staining with a combination of the IEDDA reaction and SPAAC. Scale bar: 35 μm. Reproduced with the permission from ref. 117. Copyright 2013, Wiley-VCH Verlag GmbH & Co. KGaA. (D) Schematic depiction of glycoRNA as a new class of glycosylated structures next to glycoproteins and glycolipids. Reproduced with the permission from ref. 135. Copyright 2021. Elsevier Ltd. (E) Visualization of incorporation of ManNAz into glycoRNA in mice after labeling with DBCO–biotin and staining with streptavidin–IR800 (Strep). SYBR Gold (Sybr) staining was used to visualize the total RNA level. Reproduced with the permission from ref. 135. Copyright 2021. Elsevier Ltd.

surface visualization.¹¹⁸ The influence of the different types of linkages and the size of the reporter groups on the reaction kinetics and incorporation efficiencies determined by DMB labeling were intensively studied.¹¹⁹ Another study specifically investigated the efficiencies with which different monosaccharides with different reporter groups are incorporated as sialic acids and their effect on the overall sialylation level of cells.¹²⁰ Three different galactose derivatives modified with terminal alkenes were synthesized and used to study the glycosylation of hepatic cells and the interplay with infections by *Plasmodium* parasites.¹²¹

Cyclopropenes turned out to be reporter groups with high reactivity in the IEDDA reaction and a small size, which is crucial for successful sugar incorporation. The first cyclopropene-modified sugar, 9-Cp-NeuAc,⁷² was introduced by Prescher and coworkers, and the first cyclopropene-modified ManNAc derivative, Ac₄ManNCyc,¹²² followed soon after by the Devaraj group. Alteration of the amide linkage between the cyclopropene and the sugar to a carbamate linkage resulted in a drastic increase of the IEDDA reaction rate and a new set of cyclopropene-functionalized aminosugars.^{123–125} Omitting the methyl substituent at the double bond of the cyclopropene resulted in a minimal cyclopropene reporter.⁷³ In a comparative study, different cyclopropene-modified aminosugars and their properties relevant for MGE were recently investigated by the Wittmann group.⁷⁴ Moreover,

sugars with larger reporter groups, which can be labeled by IEDDA chemistry, were synthesized and used for MGE. Norbornenes,⁷⁶ bicyclononynes,¹²⁶ and *trans*-cyclooctenes⁷⁷ are relevant when high reactivity is more important than high incorporation efficiency.

The Leeper group synthesized a set of aminosugars functionalized with primary as well as tertiary isonitriles.⁸⁰ The ManNAc derivative Ac₄ManN-*n*-Iso and the GlcNAc derivative Ac₄GlcN-*n*-Iso were used for cell–surface imaging of fixed cells after labeling through isonitrile–tetrazine ligation. Different combinations of these two derivatives with azide-modified sugars allowed the dual labeling by isonitrile–tetrazine chemistry and SPAAC.¹²⁷ The isonitrile–chlorooxime ligation was established as a bio-orthogonal ligation reaction and used for imaging of cell surface glycans of living cells as a prove of applicability of the new reaction.⁸² Cells were incubated with Ac₄ManN-*n*-Iso, reacted with a chlorooxime–biotin conjugate and stained with an avidin–dye conjugate. Additionally, dual labeling with Ac₄ManNAz labeled by SPAAC was shown.

With Ac₄ManNAcryl, the Wittmann group reported the ManNAc derivative modified with the smallest alkene reporter possible.⁹⁹ This α,β-unsaturated amide does not react with tetrazines but can be labeled by photoclick chemistry with nitrile imines generated from tetrazoles upon irradiation. The unexpected observation that a carbamate-linked methylcyclopropene had

only a low reactivity in the photoclick ligation was exploited to achieve a triple-orthogonal labeling of glycans by combination of photoclick, IEDDA, and SPAAC chemistry.⁹⁹

Friscourt and coworkers synthesized sialic acid derivatives with a chlorosydnone modification for use in MGE and subsequent labeling with a cyclooctyne.⁹⁰ Fluorescence microscopy revealed a distinct cell surface staining for cells treated with a sialic acid derivative modified in the 9 position (Neu9NSydCl). No staining was observed when cells were incubated with a sialic acid derivative with a chlorosydnone modification in the 5-position. Studies with purified enzymes showed that CMP-sialic acid synthetase does not accept the latter derivative as a substrate. Moreover, it was shown that Neu9NSydCl is preferentially incorporated by sialyltransferase ST6Gal-I over ST3Gal-IV making this derivative selective to study α 2,6-*N*-linked sialoproteins. An imidazolium-tagged mannosamine derivative, Ac₄ManN-ITag, was used to label cells non-covalently with an *N*-nitrotriacetate-dye conjugate.¹²⁸ Moreover, it was shown that glycoproteins with metabolically incorporated imidazolium tag can be enriched by ion exchange chromatography.

The Kohler group intensively studied diazirine-modified sugars for photocrosslinking.¹²⁹ A set of ManNAc derivatives, which differ in the chain length between sugar and diazirine moiety, was synthesized.¹³⁰ These reporters were used to study the interaction of glycan-binding proteins with their ligands and to covalently capture the complexes formed by cholera toxin and galectin-1.^{131,132}

Organelle-directed metabolic glycan labeling was reported using 9AzSia and the acidity-promoted accumulation of optical probes conjugated to DBCO within lysosomes.¹³³ Ac₄ManNAz was used to setup a toxicity assay for neuronal cells based on the quantification of sialic acid incorporation into cell surface glycans.¹³⁴ It turned out that the sialylation level in neurons can be used as a sensitive viability parameter that it is affected by mitochondrial respiration inhibitors even before other parameters.

Recently, Bertozzi and coworkers reported that not only lipids and proteins are glycosylated but also small noncoding RNA (Fig. 6D).¹³⁵ For discovering the existence and localization of these glycoRNAs on the cell surface, Ac₄ManNAz was used (Fig. 6E). Furthermore, it was reported that these glycans are rich in sialic acid and fucose and biosynthesized by the same machinery as *N*-glycans.

MGE can also be applied for redesigning cell surfaces, which turned out to be an efficient and robust method that can avoid genetic modification.^{136,137} Ac₄ManNAz was used as precursor for engineering cell surfaces with azides. SPAAC with DBCO-poly(hydroxyethyl acrylamide) derivatives enabled homogenous cell coating with synthetic polymers, which were stable across several cell cycles.¹³⁷ Possible future applications include cell tracking or cell-based therapies. Ac₄ManNAz was also used to label HeLa cell surfaces, followed by SPAAC with DBCO ionic probes.¹³⁸ This could decrease negative charges on cancer cell surfaces deriving from hyper sialylation. As a result of this modification, cell migration was reduced without interfering drug sensitivity.

The examples selected within this section depict the development of MGE and the subsequent detection or visualization of the modified glycans by flow cytometry and later by steadily improving fluorescence microscopy techniques. These studies highlight the opportunities of MGE to study glycans and to identify new classes of glycosylated biomolecules, such as glycoRNA.

4.2 Investigation of *O*-GlcNAcylation

The attachment of a single *N*-acetylglucosamine residue to serine or threonine side chains is called *O*-GlcNAcylation.^{139,140} This type of glycosylation is found on nearly all functional classes of intracellular proteins.¹⁴¹ The dynamic nature of *O*-GlcNAcylation arising from the transferase OGT and the glycosyl hydrolase *O*-GlcNAcase (OGA), the two only *O*-GlcNAc cycling enzymes, and its interplay with phosphorylation gives a yet complex glycosylation pattern. Earlier studies showed that the crosstalk between carbohydrates can heavily influence the incorporation of unnatural sugars as *O*-GlcNAc during MGE. It turned out that not only Ac₄GlcNAz can be used to study *O*-GlcNAcylation but also Ac₄GalNAz, which can be converted by the enzymatic machinery to UDP-GlcNAz.²⁰ The crosstalk can be suppressed by using larger reporter groups. Pratt and coworkers introduced Ac₄GlcNAalk to study *O*-GlcNAcylation and found that it results in a different incorporation pattern than Ac₄GalNAalk.¹⁴² With this new derivative, they confirmed the *O*-GlcNAcylation of the ubiquitin ligase NEDD4-1.

Later, different new sugar derivatives were synthesized and presented as more specific reporters for *O*-GlcNAcylation. Ac₃4dGlcNAz appeared to be accepted by OGT but not by OGA or glycosyltransferases involved in the biosynthesis of cell surface *N*- and *O*-glycans.¹⁴³ The use of Ac₃6AzGlcNAc allowed the identification of a variety of new *O*-GlcNAcylated proteins.¹⁴⁴ Ac₃6AzGlcNAc was also used to investigate the life time of *O*-GlcNAcylation on proteins.¹⁴⁵ This new method, relying on metabolic pulse-chase labeling, stable isotope labeling with amino acids in cell culture (SILAC), and LC-MS/MS analysis, allowed differentiation between dynamic and stable *O*-GlcNAc modifications (Fig. 7A). A set of stably *O*-GlcNAcylated proteins was found to be associated with the box C/C small nucleolar ribonucleoprotein complex. Ac₃6AzGlcNAc was chosen in this study because it is not converted to 6AzGalNAc and does not appear on the cell surface. However, this benefit comes along with an overall weaker signal intensity. Therefore, Ac₄GalNAz was used to increase labeling efficiency when the *O*-GlcNAcylation of single proteins was investigated after an immunoprecipitation.

Vocadlo and coworkers used Ac₄GalNAz in a time course metabolic feeding experiment in *Drosophila* larvae and combined it with next generation DNA sequencing to investigate the half-life and dynamics of *O*-GlcNAc on chromatin-associated proteins (Fig. 7B).¹⁴⁶ Loss of OGA activity by knock-out leads to a slight increase (about 3-fold) in half-life of these proteins. Ac₄GalNAz was also used as an *O*-GlcNAc reporter to study the role of this glycosylation during T-cell activation.¹⁴⁷ An isotope-labeled, acid cleavable biotin-alkyne conjugate was used to

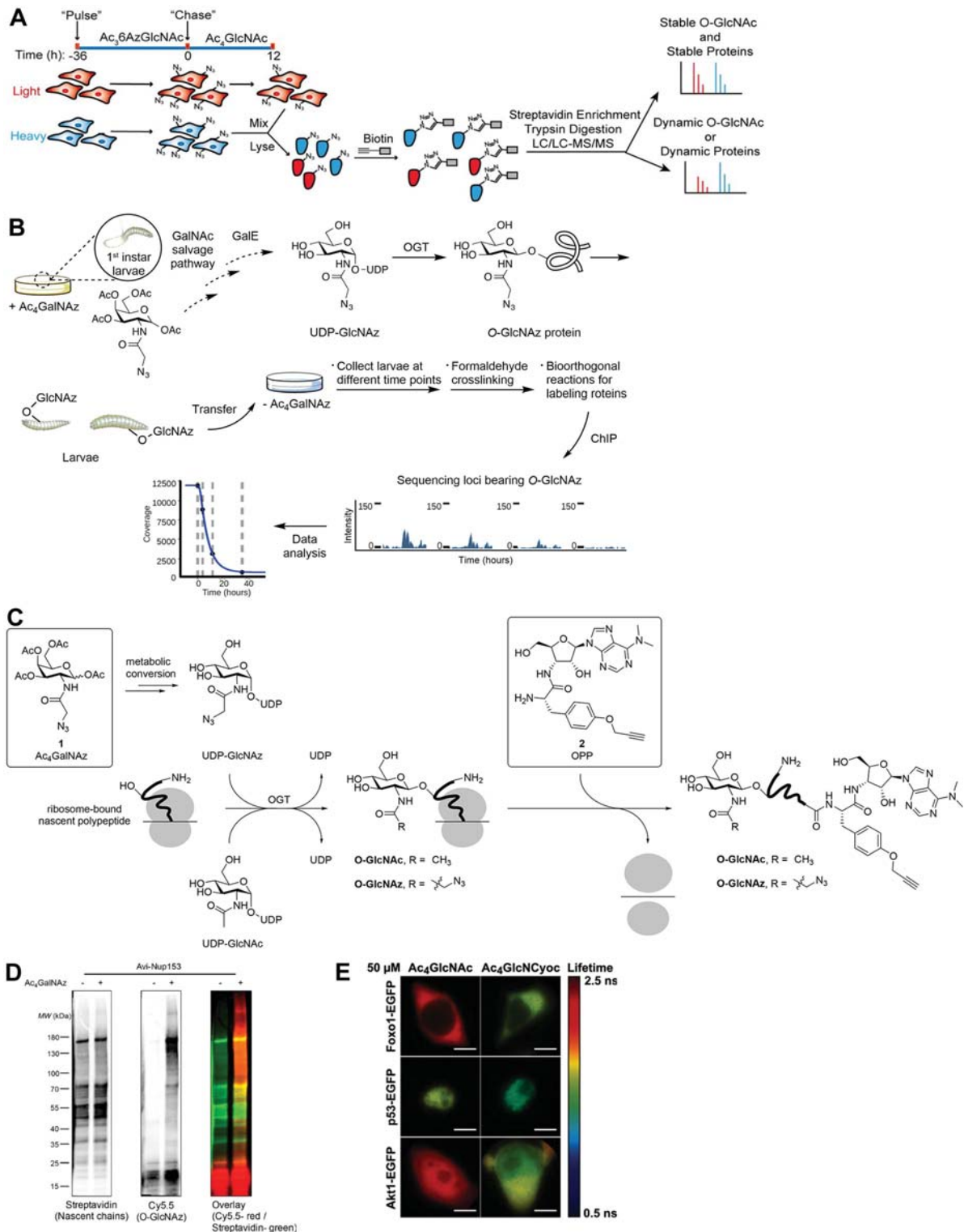


Fig. 7 (A) Schematic workflow for isotopic (heavy and light) labeling and pulse-chase feeding with $Ac_36AzGlcNAc$. After enrichment of glycoproteins, quantitative proteomic analysis is used to gather information about stability of O -GlcNAc sites. Reproduced with the permission from ref. 145. Copyright 2017, The Proceedings of the National Academy of Sciences. (B) Workflow to feed *Drosophila* larvae with $Ac_4GalNAz$ and following steps to study chromatin-associated proteins and their O -GlcNAc dynamics. Reproduced with the permission from ref. 146. Copyright 2019, American Chemical Society. (C) Workflow to obtain O -GlcNAcylated, truncated proteins released from the ribosome upon treatment with propargyl-modified puromycin (2). Reproduced with the permission from ref. 155. Copyright 2020, American Chemical Society. (D) Representative visualization of O -GlcNAcylation of truncated proteins after staining with Cy5.5, shown for avi-tagged Nup153. Reproduced with the permission from ref. 155. Copyright 2020, American Chemical Society. (E) Visualized O -GlcNAcylation of eGFP-tagged proteins in living cells by FLIM-FRET. Reproduced with the permission from ref. 78. Copyright 2016, Wiley-VCH Verlag GmbH & Co. KGaA.

enrich and prepare peptides for quantitative LC-MS/MS analysis.

The broad substrate acceptance of OGT was shown by two groups at the same time, when they introduced Ac₄2AzGlc as a reporter for *O*-GlcNAcylation.^{148,149} This derivative leads to less cell surface staining compared to Ac₄GalNAz and behaves more similar to Ac₃6AzGlcNAc.¹⁴⁹ Furthermore, it was shown that OGT can even accept UDP-Glc as a substrate.¹⁴⁸ Ac₃6AzGalNAc was also used to label mainly cytosolic and *O*-GlcNAcyated proteins.¹⁵⁰ Recently, Ac₃4FGalNAz appeared to be a precursor for an OGT substrate and interfered with the authors' plans to find a GalNAc analog as a reporter specifically for mucin-type *O*-linked glycans.¹⁵¹ Moreover, it was shown that even UDP-GalNAc can be attached to proteins by OGT making the design of selective GalNAc reporters extremely difficult.

The Vocadlo group synthesized GlcNAc derivatives that are attached to a fluorophore by different linkers.¹⁵² Even this large modification was accepted by OGA and in contrast to expectations based on the crystal structure, the derivative with the shortest linker was best accepted. For metabolic engineering in living cells, they provided an anomeric phosphorylated derivative of the fluorophore-modified GlcNAc. Fehrl and coworker reported photocaged 6AzGlcNAc-1-phosphate derivatives for a controlled, spatiotemporal release of the sugar in cells.¹⁵³

Using UDP-GlcNAz and Ac₄GalNAz, Vocadlo and coworkers discovered that *O*-GlcNAcylation plays a crucial role in stabilizing nascent polypeptide chains before they are released from the ribosome.¹⁵⁴ Specifically, they showed for the protein Sp1 that the nascent polypeptide chain is even heavier glycosylated than the mature protein and that this glycosylation prevents premature polyubiquitination and degradation by the proteasomal machinery. In following studies, the method was refined, and with a tandem metabolic labeling approach additional proteins were discovered, which are co-translationally *O*-GlcNAcyated (Fig. 7C and D).¹⁵⁵ Here, Ac₄GalNAz serves as an *O*-GlcNAc reporter and *O*-propargyl-puromycin (OPP) was used to terminate translation and release truncated proteins from the ribosome. A combination of orthogonal labeling of the sugar derivative as well as the propargyl modification of puromycin by CuAAC and two consecutive immunoprecipitation steps allowed the enrichment of *O*-GlcNAcyated truncated proteins, which could be further identified by LC-MS/MS.

The Wittmann and Zumbusch groups used Ac₄GlcNCyoc and IEDDA labeling to visualize *O*-GlcNAcylation of eGFP-tagged proteins inside living cells by FLIM-FRET microscopy.⁷⁸ With this technique, it was possible to show the localization and extent of glycosylation of a specific protein of interest. The protein p53-eGFP was detected in the nucleus and Foxo1-eGFP in the cytosol (Fig. 7E). Interestingly, Akt1-eGFP was found to be located in the cytosol as well as in the nucleus, but *O*-GlcNAcylation of the protein was increased in the nucleus as detected by a decreased fluorescence lifetime of eGFP in the nucleus compared to that in the cytosol. A similar approach was reported in fixed cells with Ac₄GalNAz as an *O*-GlcNAc reporter in combination with CuAAC¹⁵⁶ or SPAAC labeling¹⁵⁷ to visualize the glycosylation of eGFP-tagged tau and β -catenin, respectively, by FLIM-FRET microscopy.

In 2018, Chen and coworkers showed that peracetylated sugars can lead to non-specific cysteine labeling in cells,¹⁵⁸ which was later also confirmed by others.¹⁵⁹ This is especially problematic when investigating glycosylated proteins in the cytosol or in the nucleus and can lead to false positive hits for *O*-GlcNAcyated proteins. In a subsequent work, the mechanism behind this artificial *S*-glycosylation was revealed.¹⁶⁰ Anomeric deprotection of a peracetylated sugar and ring opening can promote a β -elimination of the 3-*O*-acetyl group. Subsequently, thiols can attack the so formed α,β -unsaturated aldehyde in a Michael addition leading to 3-thiolated sugars. A strategy to prevent this event is, for example, the use of 1,6-di-*O*-propionyl-GalNAz (1,6-Pr₂GalNAz), a derivative lacking the 3-*O*-acetyl group necessary for the β -elimination step.

The group further investigated the interplay of membrane permeability and the tendency to give artificial *S*-glycosylation with differently acylated GalNAz derivatives.¹⁶¹ With 1,3-di-*O*-propionyl-GalNAz (1,3-Pr₂GalNAz), the best performing sugar in this study, the *O*-GlcNAcylation and its importance for pluripotency of the embryonic transcription factor ESRRB was reported. Recently, 1,3-di-*O*-propionyl-GlcNAc (1,3-Pr₂GlcNAc) was used to identify *O*-GlcNAcyated proteins in transgenic mice expressing a mutant of UDP-GlcNAc pyrophosphorylase AGX2 in heart tissue.¹⁶² Anomerically fatty acid-modified GlcNAc derivatives were presented by the Pratt group as another possibility to prevent nonenzymatic *S*-glycosylation.¹⁶³ The fatty acid ester can be also cleaved inside cells and compensates for the increasing polarity due to the lack of acetyl groups. This makes the sugar still readily accessible by passive diffusion.

The Kohler group introduced a GlcNAc derivative with a diazirine modification, Ac₄GlcNDaz, for photocrosslinking and identification of interaction partners of *O*-GlcNAcyated proteins.¹⁶⁴ However, they could not detect the formation of UDP-GlcNDaz, when cells were cultured with the peracetylated sugar. This obstacle could be circumvented by using an anomerically phosphorylated version of the diazirine-modified sugar, Ac₃GlcNDaz-1-P(Ac-SATE)₂, in combination with a mutated version of UDP-GlcNAc pyrophosphorylase AGX1. Later, they showed that OGA does not accept *O*-GlcNDaz-modified proteins as a substrate,¹⁶⁵ and recently, an updated synthesis for phosphorylated sugar derivatives was reported.¹⁶⁶

4.3 Studying glycosyltransferases

In the last years, a new field of application of MGE emerged, which is the investigation of the substrate scope of polypeptide *N*-acetylgalactosaminyltransferases (GalNAc-Ts). The class of GalNAc-Ts is a complex family of 20 paralogs, which catalyze the first step of the formation of mucin-type *O*-glycoproteins. They can significantly differ in their substrate scope and preference, and little is known about these processes. Adapting MGE to specifically investigate GalNAc-Ts makes the following studies a good example of how chemical tools can help to answer biological questions.

The Bertozzi group developed an approach to selectively investigate the acceptor substrate of a specific GalNAc-T.¹⁶⁷ A set of UDP-GalNAc derivatives with unusually bulky azide or

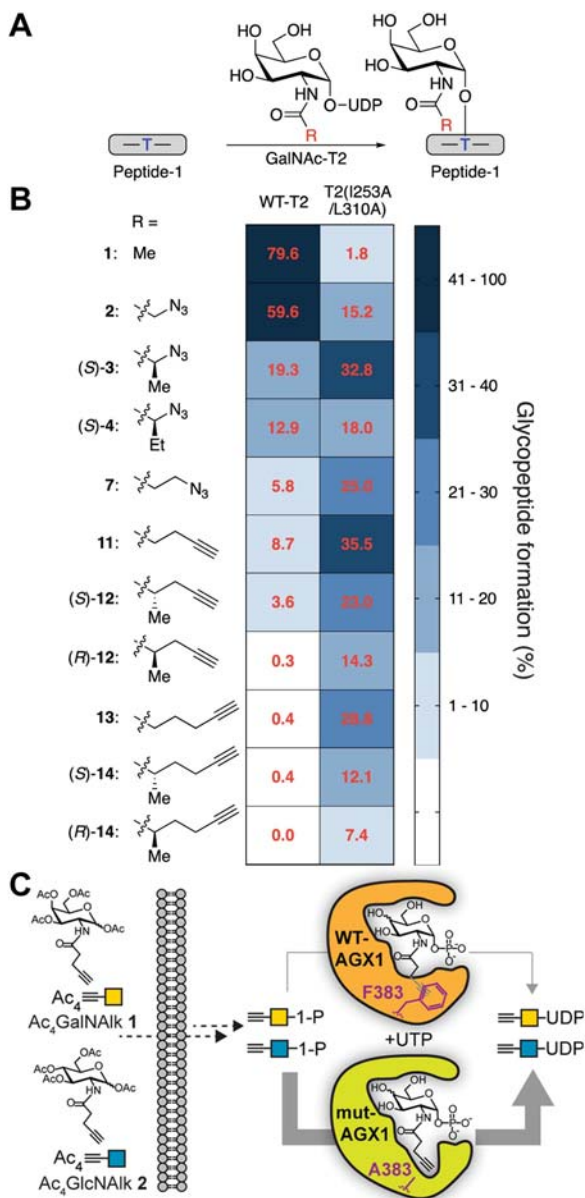


Fig. 8 (A) Illustration of the screening for an orthogonal enzyme-substrate pair for GalNAc-T2. Shown is the scheme for the glycosylation reaction with a model peptide to obtain information about GalNAc-T2 activity with different modified UDP-GalNAc derivatives. Reproduced with the permission from ref. 167. Copyright 2019, American Chemical Society. (B) Influence of different residues in the *N*-acetyl position on the efficiency of the glycosylation reaction shown in A. Reproduced with the permission from ref. 167. Copyright 2019, American Chemical Society. (C) Illustration of the metabolic bottleneck AGX1 and how a mutated version of this enzyme can lead to a more efficient production of alkyne-modified UDP-sugars. Reproduced with the permission from ref. 170. Copyright 2019, American Chemical Society.

alkyne modifications in the *N*-acetyl position was tested with the goal to find a compound, which is not accepted by wild-type GalNAc-Ts (Fig. 8A and B). Then, the binding pocket of a GalNAc-T was mutated to accept the bulky modification. At the same time, the mutated enzyme lost the affinity for the natural substrate UDP-GalNAc. Screening of enzyme activity

and turnover rates resulted in a mutated enzyme with good activity for the new bulky substrate. The setup was tested with model peptides as acceptor substrates originating from known *O*-glycosylated proteins. The described method was further developed to be used in cells to identify proteins, which are glycosylated by GalNAc-T1 or GalNAc-T2.¹⁶⁸ The mutated enzyme was expressed in cells and the expression platform was proofed to be functional with bulky alkyne modified GalNAc derivatives. To deliver the substrate in living cells, the GalNAc derivative was anomericly phosphorylated to allow successful biosynthesis of the corresponding UDP-GalNAc derivative. With an acid-labile biotin-azide conjugate, glycoproteins were enriched and identified by LC-MS/MS analysis.

In a similar work, a bulky azide-modified GalNAc derivative (GalNAzMe), which is not converted into the GlcNAc derivative by the epimerase GALE, was designed.¹⁶⁹ To use this sugar derivative in living cells, it was again applied as an anomericly phosphorylated derivative in combination with a mutated pyrophosphorylase AGX1. In this way, a more precise carbohydrate derivative for MGE was obtained to investigate *O*-linked GalNAc glycosylation. Furthermore, the derivative was used for high-resolution imaging of the cell surface and imaging of organoids.

Schumann and coworker identified the pyrophosphorylase AGX1 as the metabolic bottleneck of the GalNAc and GlcNAc salvage pathways.¹⁷⁰ AGX1 catalyzes the formation of UDP-GalNAc from GalNAc 1-phosphate and UTP and UDP-GlcNAc from GlcNAc 1-phosphate and UTP, respectively. This bottleneck was shown to be responsible for the inefficient incorporation of the alkyne derivatives Ac₄GalNAik and Ac₄GlcNAik. A mutated version of AGX1 improved the incorporation for better cell surface imaging and showed a different labeling pattern compared to the azide derivatives Ac₄GalNAz and Ac₄GlcNAz (Fig. 8C). Another study compared the ionization efficiency and fragmentation behavior of synthetic glycopeptides with azide- or alkyne-modified GalNAc derivatives after bioorthogonal derivatization with different tags.¹⁷¹

4.4 Modification of the extracellular matrix

The extracellular matrix (ECM) is part of tissue structures especially occurring in conjunctive tissue and responsible for the organization and stability of tissue.¹⁷² It is located in the intercellular space and built up by fibrous proteins and glycosaminoglycans (GAGs). Moreover, the ECM has not only structure-giving capabilities but also other functions including signal transduction between cells, morphogenesis, cell differentiation and homeostasis.^{173,174} The ECM can be used to generate cell-derived matrices (CDM), which can serve as biomaterial for application in regenerative medicine, 3D cell culture or for studying cell and tissue physiology.^{175,176} Although CDMs are good mimics of cellular or tissue environments, the absence of specific targeting functionalities can be adverse. Engineering the ECM by MGE provides options for altering properties of the resulting CDM. The generation of such functionalized ECMs can be achieved by cultivating fibroblasts¹⁷⁷ or mesenchymal stem cells¹⁷⁸ in presence of synthetic sugar derivatives. These cell

types then produce a lucrative amount of ECM decorated with bioorthogonal reporter groups. The obtained so-called *click*-ECM¹⁷⁷ can be used for several applications. ECM functionalized with azide groups derived from Ac₄GalNAz was conjugated with an alkyne-fluorophore probe or with surface-bound cyclooctynes to achieve a covalent coating with *click*-ECM.¹⁷⁷ Labeling with alkyne-biotin enables a variety of functionalization due to many commercially available streptavidin probes. Ac₄GlcNAz was used to modify the ECM network derived from NIH 3T3 fibroblasts.^{179,180} Moreover it was also possible to conjugate a therapeutic peptide inhibitor against myostatin to the azide-modified ECM.^{179,180} Recently, it was shown that cyclopropenes are suitable reporter groups for the generation of an ‘advanced *click*-ECM’ that can be further functionalized by the IEDDA reaction.¹⁸¹

4.5 Cancer targeting

Cancer cells differ in their metabolism in comparison to healthy cells. In cancer cells, most proliferation mechanisms are out of control leading to uncontrollable growth. An increased metabolism and altered morphology are some consequences thereof. Cancer cells often show higher glycosylation levels; especially sialic acids, branched cell surface glycosylation, and core fucosylation are overrepresented.^{182,183} These changes in cell surface glycosylation can promote cancer cell dissociation and invasion, influence extracellular stimuli responses, and can alter various interactions between cells or responses to external signals. Considering that MGE is a suitable method for the visualization of cell-surface glycosylation, it is also a potential tool for cancer diagnostics and therapy.

Cancer cell-specific drug delivery of cytotoxic agents requires a high degree of specificity. Direct injection of modified carbohydrate derivatives into tumor tissue of mice can achieve an effective and specific targeting exploiting MGE. However, this strategy is only applicable for solid and easily accessible cancer tissue. Systemic delivery strategies, in which the sugar derivative is encapsulated or cancer cell-specifically modified, are alternative ways to achieve delivery and uptake into cancer cells. In the following, we present selected approaches covering different tumor targeting strategies to achieve tumor visualization and therapy *in vitro* and *in vivo*.

4.5.1 Exploitation of cancer cell-specific metabolism. To achieve modification of cell surface glycan structures with azide functionalities, mice were injected with Ac₄GalNAz (Fig. 9A).¹⁸⁴ Subsequent treatment with a gadolinium-containing bioorthogonal magnetic resonance imaging (MRI) probe with a TMDIBO residue enabled labeling of the cell surface of azide-presenting cells and thereby tomographical imaging of tumor glycosylation *in vivo* (Fig. 9B). However, the probe showed also labeling of other tissues, such as pancreas, liver, and spleen. Recently, intravenous injection of Ac₄ManNAz into mice showed a higher incorporation of azide groups on the cell surface of lung and breast cancer cells, in comparison to other tissues.¹⁸⁵ Labeling of these azide-presenting cancer cells with DBCO-Pam₃CysSer(Lys)₄ (Fig. 9C) led to a neoantigen presentation on the cell surface. Pam₃CysSer(Lys)₄ is a synthetic lipopeptide, which activates cellular pro-inflammatory processes. Establishing a tumor-specific antigen circumvents

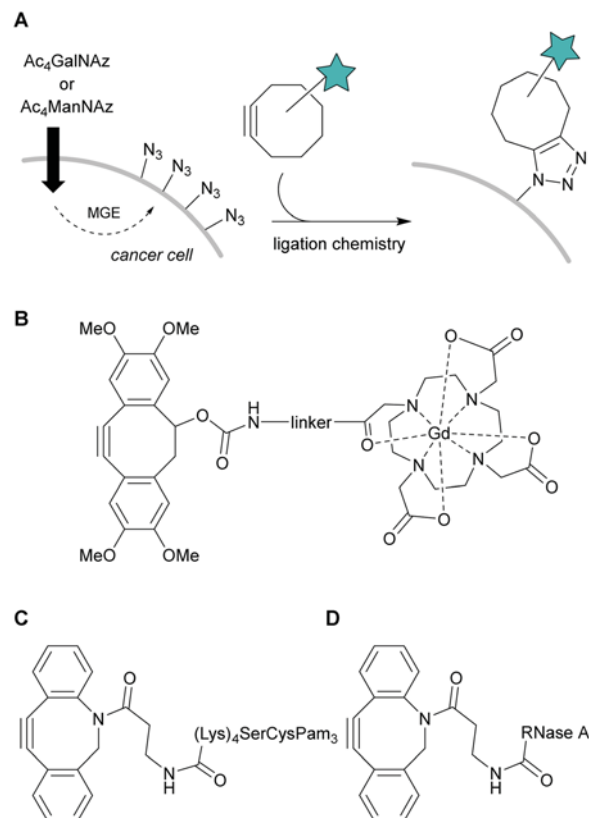


Fig. 9 Modification of cancer cell surface glycans. (A) Uptake and metabolism of Ac₄ManNAz or Ac₄GalNAz by cancer cells. Cell surfaces present azide functionalities, which enable further derivatization by SPAAC with cyclooctyne moieties. (B) TMDIBO-MRI probe for tomographical imaging of tumor glycans.¹⁸⁴ (C) DBCO-Pam₃CysSer(Lys)₄ leads to neoantigen presentation on cancer cells.¹⁸⁵ (D) DBCO-RNase A as an example for a cytosolic protein, which can be delivered to cancer cells.¹⁸⁶

immunological tolerance against many cancer types and antigens. However, possible off-target effects cannot be excluded.

MGE was also used as part of a cytosolic protein delivery strategy (Fig. 9D).¹⁸⁶ DBCO-modified proteins, including RNase A, cytochrome *c*, and bovine serum albumin, were clicked to azide-presenting tumor cells. Bringing the target cargo in direct proximity to the cell membrane led to an efficient internalization by the azide-labeled cancer cells. Since the internalized RNase A largely retained its enzymatic activity, tumor growth in mice was slowed down after intratumoral injection of Ac₄ManNAz and labeling with DBCO-RNase A. Another strategy to label glycoengineered tumor cells is the use of a photosensitizer conjugated to DBCO.¹⁸⁷ This enabled a more efficient radio-dynamic therapy after X-ray irradiation in tumor bearing mouse models.

A different strategy was reported in 2015, where the tumor-associated carbohydrate antigen (TACA) GM3 was engineered to contain the artificial structure *N*-phenylacetyl neuraminic acid instead of the natural *N*-acetyl neuraminic acid at the end of this glycan structure (Fig. 10A).¹⁸⁸ TACAs are one of the most abundant tumor-associated antigens present on the cell surface of cancer cells and are recognized by the immune system.^{189,190}

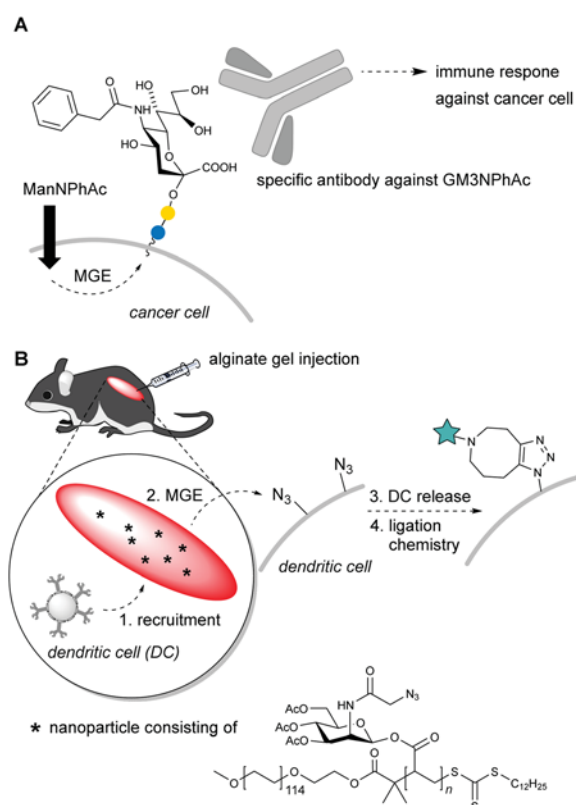


Fig. 10 MGE for cancer treatment. (A) Glycoengineered cancer cells present an artificial GM3 carbohydrate structure, which can be recognized by specific antibodies against GM3NPhAc and thereby induce immune response.¹⁸⁸ (B) Nanoparticles consisting of azide-modified ManNAc derivatives were implemented in an alginate gel. After gel injection into mice, dendritic cells were recruited to the gel and labeled with azides within the gel structure. Dendritic cells can be released from the gel and ligated via SPAAC *in vivo*.¹⁹²

However, immunological tolerance against TACAs of some cancer cells is an increasing problem. A combination of MGE and dendritic cell vaccination was a possible strategy to overcome this obstacle.¹⁸⁸ *N*-Phenylacetyl-*D*-mannosamine was used as a precursor of the corresponding sialic acid and was intraperitoneally injected into mice. Engineered cancer cells presented the artificial carbohydrate structure named GM3NPhAc on their surface. Mouse bone-marrow-derived dendritic cells were pulsed with a short peptide sequence conjugated to GM3NPhAc leading to antigen presentation on the cell surface. Vaccination of mice with these carbohydrate-pulsed dendritic cells lead to the development of GM3NPhAc-specific antibodies. These antibodies were able to promote an immune response and thereby retard tumor growth and metastasis. Previous work showed that ManNPhAc is a suitable sialic acid precursor, which can be used for *in vitro* and *in vivo* modification of cancer cells but not normal cells.¹⁹¹ In the mouse model, neither an autoimmune reaction against healthy cells nor ManNPhAc treatment-related toxicity was observed.

In a different approach, dendritic cells were metabolically glycoengineered with azide functionalities, allowing the labeling of these cells with different DBCO conjugates.¹⁹² This modification of

dendritic cells enabled their tracing in mice or promoting an immune response against tumor cells *in vivo*. Hereby, an alginate gel structure was injected into mice (Fig. 10B). Dendritic cells were recruited to this pore-forming gel as it released colony-stimulating factors for dendritic-cell enrichment. For the azide modification, a triacetylated mannosamine precursor was used and released within the gel structure to enable selective engineering of the dendritic cells. The sugar derivative was additionally modified with poly(ethylene glycol) methyl ether 2-(dodecylthiocarbonothioylthio)2-methylpropionate (PEG DDMAT) at the anomeric position to improve water solubility and increase release efficiency from hydrogels. The system allowed the controlled modification and release of azide-presenting dendritic cells. Functionalized dendritic cells were then successfully conjugated to tumor antigens, adjuvants, cytokines, and other immunomodulatory agents.

Sialic acid-binding immunoglobulin-like lectins (Siglecs) are immunomodulatory receptors present on the surface of immune cells. Interactions between Siglecs and sialic acids play an important role in immune system regulation, and dysfunctions in this interaction can promote cancer progression or autoimmune diseases. Using MGE and subsequent bioorthogonal ligation by CuAAC, sialic acids on the surface of living cells were engineered resulting in altered binding affinity to Siglecs.¹⁹³ Screening of a library of glycoengineered cells uncovered modifications with dramatically increased Siglec binding affinity of more than 100-fold. Glycoengineered cells showed an immunosuppressive behavior, which might be applicable in dampen the immune response in autoimmune disease.

4.5.2 Exploitation of the enhanced permeability and retention effect. Nanoparticles with a size range of 10–200 nm are known to penetrate tumor vasculature.¹⁹⁴ This phenomenon is called *enhanced permeability and retention* (EPR) effect and can be utilized as targeting strategy. However, the targeting effect of this system is limited due to unspecific accumulation of nanoparticles in off-target tissues, as for example liver and spleen.¹⁹⁵ The system can be improved by a combination of MGE and bioorthogonal chemistry. Intratumoral administration of Ac₄ManNAz into mice has been shown to enable an effective accumulation of intravenously injected DBCO-liposomes to cancer cells by using bioorthogonal chemistry (Fig. 11A).¹⁹⁶ Significant tumor targeting of DBCO-liposomes containing a near infrared fluorescence (NIRF) dye, could be observed in tumor tissue (Fig. 11B).¹⁹⁶ In comparison to traditional targeting strategies, such as targeting peptide-sequences, the use of DBCO-liposome nanoparticles in combination with MGE and bioorthogonal chemistry showed a greater targeting capability of nanoparticles to cancer cells.¹⁹⁷ Another nanoparticle-based strategy used a DBCO nanoprobe, which encapsulated a near infrared dye to enable photo thermal therapy of azide-presenting tumor cells successfully in a murine model.¹⁹⁸

Immobilizing a high number of ManNAz molecules on a generation 4 poly(amidoamine) dendrimer (nano-MPs) *via* ester bonds to the hydroxy group in the 6-position of ManNAz led to release of the sugar and presentation of azides on heterogeneous tumor cells *in vitro*.¹⁹⁹ Selectivity was generated due to

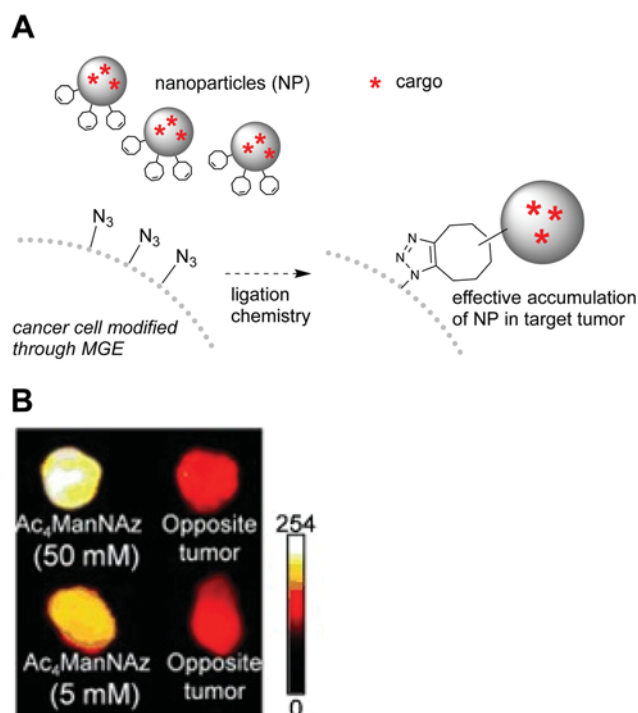


Fig. 11 Cancer targeting exploiting the EPR effect and MGE. (A) After MGE, tumor cells present azides on the cell surface, which enables tumor targeting of nanoparticles by bioorthogonal ligation. (B) NIRF images of *ex vivo* tumor tissue after treatment with Ac₄ManNAz or control tumors without sugar treatment. After intravenous injection of DBCO–liposomes containing a NIRF dye, tumor groups showed more intense NIRF signal in a sugar concentration-dependent manner. Reproduced with the permission from ref. 196 Copyright 2012, Wiley-VCH Verlag GmbH & Co. KGaA.

the EPR effect arising from the nano-sized structure of the dendrimer and the higher metabolism of cancer cells. Control experiments with nano-MP-treated liver tissue showed a minor amount of azide functionalities in comparison to tumor tissue. Nano-MP injection into mice showed a successful generation of azide groups in the target tumor tissue, whereas injection of Ac₄ManNAz was less effective.

Moreover, sugar reporters can be encapsulated in ligand-targeted liposomes to address tumor cells (Fig. 12A).²⁰⁰ The liposomes were modified with ligands for epitopes found on the target cells. Upon binding, the cargo was released and the azidosugar 9AzSia, which was used in this study, was incorporated into cell surface glycans. This kind of targeted metabolic glycan labeling enhanced the delivery efficiency of sugar reporters for applications in cell-specific or tissue-specific imaging or detection.

The EPR effect can additionally be enhanced by using glycol chitosan, which increases membrane permeability and leakage of tumor cells further.²⁰¹ Intravenous injection of glycol chitosan nanoparticles into mice delivered Ac₄ManNAz to cancer cells and enabled the decoration of tumor cells with azide moieties on the cell surface (Fig. 12B). Using cyclooctyne-modified nanoparticles containing anti-cancers drugs, the cargo was delivered specifically to azide-presenting cancer cells *in vivo*. Conjugated glycol chitosan nanoparticles were also used for a dual-modal stem cell imaging approach.²⁰²

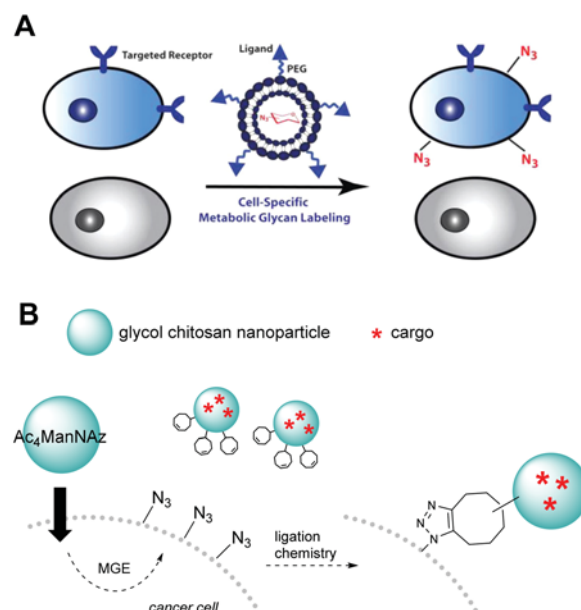


Fig. 12 Nanoparticle-based targeting. (A) Ligand-targeted liposomes deliver 9AzSia selectively to cells presenting corresponding receptors on their cell surface. Reproduced with the permission from ref. 200 Copyright 2012, American Chemical Society. (B) Glycol chitosan nanoparticles can enhance Ac₄ManNAz uptake by tumor cells due to the EPR effect. In combination with bioorthogonal click chemistry, cargos encapsulated in nanoparticles, such as anticancer drugs, can be selectively addressed to tumor cells.²⁰¹

The use of cell membranes as nanoparticle mimics has several advantages including their excellent biocompatibility and versatile functionality.²⁰³ T cells are promising for tumor-targeting since immune recognition receptors on the cell surface can be used for this purpose.²⁰⁴ However, this targeting strategy has to overcome problems related to the heterogeneity of some tumors. To improve the targeting efficacy, T cell membranes were modified with azide groups by MGE (Ac₄GalNAz).²⁰⁵ Fluorescently labeled nanoparticles coated with azide-labeled T cell membranes targeted BCN-presenting tumor tissue of mice through immune recognition and bioorthogonal chemistry. Fluorescence intensity in the tumor was 1.5-fold compared to mice that were treated with unmodified T cell-coated nanoparticles.

Extracellular vesicles (EVs) are membrane particles that are secreted by nearly every cell type. They are important for inter-cellular interactions and for the transport of biomolecules.²⁰⁶ These properties enable the use of EVs as diagnostic biomarkers and therapeutic nanomedicines. However, the direct targeting to the desired destination is challenging. Using MGE to modify these EVs by treatment of the donor cells with Ac₄ManNAz and labeling these cells with a DBCO-polyethyleneglycol-hyaluronic acid conjugate led to surface-edited EVs.²⁰⁷ This modification enabled a directed recruitment to hyaluronic acid receptors, which are present on tumor cells, and thereby enabled receptor-mediated endocytosis. *In vivo* tests in mice showed that edited EVs exhibited high targeting efficiency and a longer half-life in the bloodstream.

4.5.3 Cancer targeting with glycoengineered immune cells.

Immune cells are able to kill cancer cells, however, most of them lack tumor-specific targeting capabilities.²⁰⁸ Since engineering of immune cells can be achieved by MGE *in vitro*, it is possible to label immune cells by bioorthogonal chemistry with ligands that are recognized by cancer-specific receptors (Fig. 13A). Using this strategy, various approaches showed an improved recruitment of these modified immune cells to the tumor after injection into mice (Fig. 13B).

Natural killer (NK) cells are one example of very potent immune cells with high anti-cancer activity, but insufficient tumor-targeting properties. To overcome this restriction, NK cells were labeled by MGE with an altered ligand for CD22, a receptor belonging to the Siglec family.²⁰⁹ CD22 receptors are found on the surface of B-lymphoma cells. The natural ligand for this cancer marker is the trisaccharide Neu5Ac α 2-6Gal β 1-4GlcNAc. To modify the natural CD22 ligand, MGE was carried out in NK cells with a sialic acid derivative modified with a benzoate amide at the 9 position of sialic acid (Fig. 14A). This modification significantly enhances the binding affinity towards CD22.²¹⁰ The glycoengineered NK cells showed a higher affinity and an enhanced killing activity for CD22-presenting cells *in vitro* and *in vivo* (Fig. 14B and C).²⁰⁹

Recently, NK cell surfaces were decorated with azide functionalities *via* MGE using 9-azido *N*-acetyl neuraminic acid methyl ester.²¹¹ The tumor-targeting capacity was improved by bioconjugation of DBCO-modified cetuximab to the azide groups presented on the NK cell surface. Cetuximab is an antibody, which is specific for the epidermal growth factor receptor, and it is widely used in cancer immunotherapy. In comparison to non-functionalized control NK cells, the

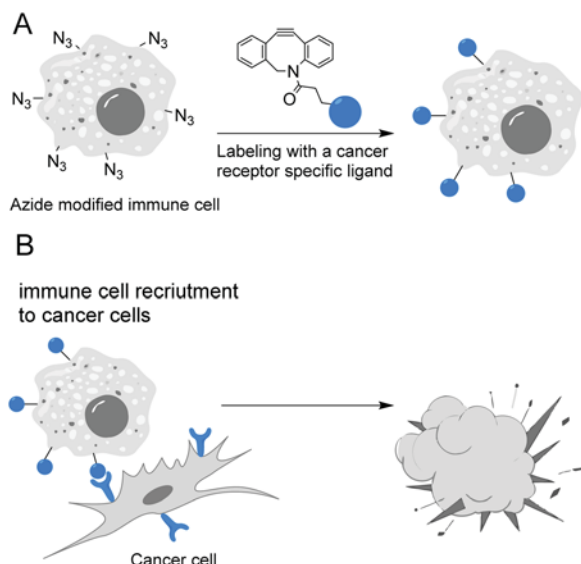


Fig. 13 Cancer targeting with glycoengineered immune cells. (A) Immune cells are treated with azide-modified sugar derivatives to enable artificial functionalization of the cell surface. After bioorthogonal ligation reaction with DBCO conjugates, the immune cells present, for example, a cancer-specific receptor ligand. (B) The modified immune cells can be recruited to cancer cells leading to cancer cell death.

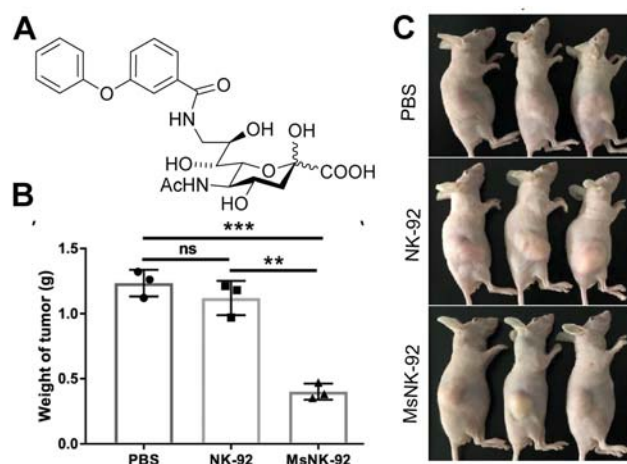


Fig. 14 (A) sialic acid with benzoate modification to modulate the natural CD22 ligand on NK cells. (B) Tumor weight measurements of mice after treatment with untreated NK cells (NK-92), metabolically engineered NK cells (MsNK-92) or PBS as control. Tumor growth was slowed after treatment with the modified NK cells. Reproduced with the permission from ref. 209. Copyright 2020, American Chemical Society. (C) Images of mice with tumors after different treatments. Mice, that were treated with the engineered NK cells showed smaller tumors in comparison to mice, that were treated with normal NK cells. Reproduced with the permission from ref. 209. Copyright 2020, American Chemical Society. <https://pubs.acs.org/doi/10.1021/acscentsci.9b00956>.

functionalized NK cells showed a significantly enhanced protection against tumor development in a mutant mouse cancer model, which is resistant to direct cetuximab treatment.

Genetically modified T cells can also be used in cancer therapy.^{212,213} The common transduction of T cells *via* viral vector systems can be improved by combining it with MGE and bioorthogonal chemistry. DBCO was immobilized on lentiviruses leading to an effective binding of the virus to azide presenting T cells and thereby a more efficient uptake of the vector.²¹⁴

4.5.4 Cancer cell-specific uncaging of metabolic precursors.

Based on the idea of prodrug strategies, in which caged drugs are administered to improve not only bioavailability but also target-specific drug release, MGE reporters have been developed that are metabolized in a cancer cell-specific manner. These sugar derivatives are protected by functionalities that are only cleaved by enzymes that are overexpressed in cancer cells. Once liberated within the cancer cell, the sugars are further metabolized and incorporated into the cancer cell glycans. In 2010, the Bertozzi group used this strategy for the first time in MGE.²¹⁵ Ac₄ManNAz was modified in the 6-position with a peptide sequence specific for prostate-specific antigen protease, a serine protease that is highly upregulated in prostate cancer. Living cells were stained in a two-step procedure with a DIFO-biotin and a quantum dot 605-streptavidin conjugate.

Cathepsin B is a cysteine protease that is abundant in the cytoplasm of various tumor cells. Accordingly, a cathepsin B-specific cleavable peptide sequence (Lys-Gly-Arg-Arg, KGRR) was connected *via* a *p*-aminobenzyloxycarbonyl linker to the 6-hydroxy group of Ac₃ManNAz (Fig. 15A).²¹⁶ After cellular

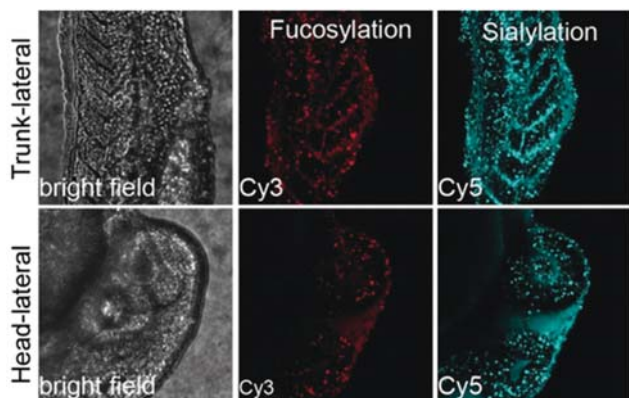


Fig. 16 Lateral view of zebrafish embryos injected with Cy3-modified GDP-Fuc and Cy5-modified CMP-Sia. Reproduced with the permission from ref. 229. Copyright 2019, Wiley-VCH Verlag GmbH & Co. KGaA.

improve the imaging and cell labeling of stem cells. After stem cell transplantation into mice, the cell migration of the labeled stem cells could be observed from the transplanted area to brain stroke areas through magnetic resonance imaging. Adipose-derived mesenchymal stem cells were also used for stem cell-based therapy for liver diseases.²²⁰ The success of such therapies heavily relies on the number of cells that are delivered to the injured liver tissue. One approach to improve this, is to use MGE to label the adipose-derived mesenchymal stem cells with liver-target peptide structures *via* SPAAC (DBCO-conjugates).²²¹ The labeling increases the binding affinity of the modified stem cells for liver tissue significantly *in vitro* and *in vivo*. In combination with infrared dye conjugates, it was also possible to track the injected stem cells in a mouse model.

Tissue engineering is a promising tool for replacing or repairing injured tissue or organs.²²² In this approach, donor cells are expanded and subsequently cultured on a temporary scaffold. One drawback of these artificial scaffolds is the lack of biological guidance signals resulting in poor *in vivo* cellularization. To overcome this limitation, a bioorthogonal labeling strategy using a DBCO-modified polymer film has been developed.²²³ Macrophages were labeled with azides by MGE and subsequently seeded on the DBCO-modified scaffold resulting in covalent attachment to the scaffold. The material showed good biocompatibility and could be implanted in mice.

Telomerase-immortalized human mesenchymal stromal cells (hMSC-TERT) were successfully labeled with different azide-modified aminosugars without interrupting the cell differentiation behavior *in vitro*.²²⁴ This allowed a more detailed investigation of glycosylation processes during skeletal development. MGE was also used to protect insulin-producing pancreatic β cells.²²⁵ During type 1 diabetes, a chronic autoimmune disease, these cells are destroyed by autoreactive T cells. In a new translational approach based on MGE, β cells were engineered with Ac₄ManNAz and conjugated to DBCO-modified co-inhibitory immune checkpoint molecules, which protect β cells against autoreactive T cells by inducing antigen-specific immunotolerance.

4.7 MGE in higher organisms

The first application of MGE in living animals was reported in 2004, when Bertozzi and coworkers used Ac₄ManNAz to chemically remodel cell surfaces in mice.⁴² Labeling of the azides was achieved by Staudinger ligation with a Flag peptide-labeled phosphine either *ex vivo* using isolated splenocytes or even *in vivo*. Since then, MGE has been carried out numerous times in mice as discussed in the previous sections.

4.7.1 Zebrafish. In 2008, Bertozzi and coworkers used Ac₄GalNAz to study the glycosylation in developing zebrafish.²²⁶ Zebrafish embryos were incubated with unnatural sugar and labeled by SPAAC with different DIFO-dye conjugates at different time points allowing a spatiotemporal analysis of mucin-type O-glycans during development. In another study, MGE with Ac₄GalNAz was combined with additional labeling of sialic acids by oxidizing the sialic acids with sodium periodate and labeling with an oxamine-dye conjugate.²²⁷ Later, the visualization of fucosylated glycans in zebrafish after microinjection of GDP-Fuc6Az into the embryo and staining by SPAAC with a DIFO-dye conjugate was reported.²²⁸ A cyclooctyne-modified sialic acid derivative, BCNSia, and its labeling by IEDDA reaction with a tetrazine-dye conjugate enabled the visualization of sialylated glycans in living zebrafish embryos.¹²⁶ Wu and coworkers showed that a fluorophore-tagged CMP-sialic acid derivative and GDP-fucose derivatives delivered by microinjection were incorporated into glycan structures in zebrafish embryos (Fig. 16).²²⁹ The direct attachment of the fluorophore to the sugar allowed the trafficking of the sugar probes and their turnover. An alkyne-modified UDP-Gal derivative, UDP-6AlGal, delivered by microinjection was found to be incorporated into N-glycans in zebrafish embryos and allowed to study glycoproteins, the glycan structure as well as the responsible glycosyltransferases.²³⁰

4.7.2 Plants. The origin of most monosaccharides in living organisms is the oxygenic photosynthesis. Whereas mammals are dependent on carbohydrate supply by ingestion, plants are able to produce hexoses by sunlight and CO₂. Plants have, in comparison to animals, additional saccharides to build up structural elements, such as their cell wall. Conventional methods for cell wall imaging have several drawbacks, like the usage of antibodies, which are only specific for various glycan epitopes. MGE is a suitable tool for imaging plant structures, even in living plants.²³¹ First, FucAl was successfully incorporated into *Arabidopsis* roots.²³² This gave new insights into the development of pectin structures. Screening various sugar reporters showed different aptitudes for their application in plant cell labeling.²³³ Ac₄FucAl, Ac₄FucAz, Ac₄Me8AzKdo, Ac₄GlcNAz, and Ac₄GalNAz and Ac₄GlcNCp lead to robust staining after labeling with a fluorescence dye in *Arabidopsis* roots. Later, various monosaccharides, like N-acetylglucosamine, N-acetylgalactosamine, L-fucose, and L-arabinofuranose bearing azide groups, were used in MGE experiments in *Arabidopsis*.²³⁴ In combination with IEDDA sugar reporters, dual labeling in plant cells was possible. In a triple labeling approach, SPAAC, CuAAC, and IEDDA were used to investigate cell wall formation. Among other reporters, an alkyne fucose derivative was employed.²³⁵ 3-Deoxy-D-manno-oct-2-ulosonic acid (Kdo) is part of a cell wall pectin. Azide modified

Kdo in combination with click chemistry was used for *in muro* visualization.²³⁶ Tobacco or *Arabidopsis* seedlings were incubated with the sugar reporter and afterwards labeled with a dye. These MGE experiments represent a tool for the investigation of synthesis and redistribution of cell wall pectins. Besides acting as structure-giving elements (e.g. as cell wall components), carbohydrates are also present as *N*-glycans on plant proteins. Ac₄GlcNAz can be used to visualize this *N*-glycan structures after labeling with an alkyne–dye conjugate *via* Cu-click chemistry.²³⁷ This gives a hint to the presence of a GlcNAc salvage pathway in plants.

5. Conclusions

Three decades after the first publications of the Reutter group on the metabolization of ManNAc derivatives with a modified *N*-acetyl side chain by the enzymes of the sialic acid biosynthesis pathway, MGE has evolved into a mature technique to visualize glycan structures in cells and even whole organisms or to isolate glycoconjugates after attachment of a suitable probe by bioorthogonal chemistry. More recently, targeting strategies based on bioorthogonal ligation after MGE have been realized even in living animals providing promising new approaches for selective drug delivery and tumor diagnosis. Despite these achievements, several challenges remain to be addressed by future research. These include (i) the development of more selective carbohydrate derivatives that end up as the desired sugar and at the desired site of modification within glycoconjugates and do not lead to unspecific labeling, for example artificial *S*-glycosylation, (ii) the development of improved carbohydrate derivatives that can be derivatized by suitable ligation chemistries inside living cells without toxic catalysts and the components of which are not attacked by thiols present inside cells in high concentrations, and (iii) the improvement and extension of cell type- and tissue-specific targeting strategies. Further exiting developments of MGE can be expected in future.

Author contributions

LMH and MK contributed equally and either has the right to list herself or himself first in bibliographic documents. All authors contributed to the conception of this review, writing of the manuscript, revision, and approved the final version.

Conflicts of interest

There are no conflicts to declare.

Acknowledgements

This work was supported by the Deutsche Forschungsgemeinschaft (SFB 969, project B05; SPP 1623), the Ministerium für Wissenschaft, Forschung und Kunst Baden-Württemberg (33-7533-7-11.9/7/2), and COST Action GLYCONanoProbes (CA18132).

References

- 1 *Essentials of Glycobiology*, ed. A. Varki, R. D. Cummings, J. D. Esko, P. Stanley, G. W. Hart, M. Aebi, D. Mohnen, T. Kinoshita, N. H. Packer, J. H. Prestegard, R. L. Schnaar and P. H. Seeberger, Cold Spring Harbor Laboratory Press, Cold Spring Harbor, NY, 4th edn, 2022.
- 2 R. Apweiler, H. Hermjakob and N. Sharon, *Biochim. Biophys. Acta*, 1999, **1473**, 4–8.
- 3 G. A. Houry, R. C. Baliban and C. A. Floudas, *Sci. Rep.*, 2011, **1**, 90.
- 4 X.-L. Sun, *Glycobiology*, 2021, **31**, 1245–1253.
- 5 J. Zhang, R. E. Campbell, A. Y. Ting and R. Y. Tsien, *Nat. Rev. Mol. Cell Biol.*, 2002, **3**, 906–918.
- 6 The technique has originally been termed metabolic oligosaccharide engineering (MOE). However, since not only glycans consisting of several monosaccharides (*i.e.*, oligosaccharides) can be engineered but also glycoforms consisting of a single monosaccharide (*O*-GlcNAcylated proteins), we prefer to use the more general term metabolic glycoengineering (MGE).
- 7 O. T. Keppler, R. Horstkorte, M. Pawlita, C. Schmidt and W. Reutter, *Glycobiology*, 2001, **11**, 11R–18R.
- 8 D. H. Dube and C. R. Bertozzi, *Curr. Opin. Chem. Biol.*, 2003, **7**, 616–625.
- 9 H. Kayser, R. Zeitler, C. Kannicht, D. Grunow, R. Nuck and W. Reutter, *J. Biol. Chem.*, 1992, **267**, 16934–16938.
- 10 L. K. Mahal, K. J. Yarema and C. R. Bertozzi, *Science*, 1997, **276**, 1125–1128.
- 11 K. K. Palaniappan and C. R. Bertozzi, *Chem. Rev.*, 2016, **116**, 14277–14306.
- 12 T. J. Sminia, H. Zuillhof and T. Wennekes, *Carbohydr. Res.*, 2016, **435**, 121–141.
- 13 P. R. Wratil, R. Horstkorte and W. Reutter, *Angew. Chem., Int. Ed.*, 2016, **55**, 9482–9512.
- 14 P. A. Gilormini, A. R. Batt, M. R. Pratt and C. Biot, *Chem. Sci.*, 2018, **9**, 7585–7595.
- 15 C. Agatemor, M. J. Buettner, R. Ariss, K. Muthiah, C. T. Saeui and K. J. Yarema, *Nat. Rev. Chem.*, 2019, **3**, 605–620.
- 16 J. A. Prescher and C. R. Bertozzi, *Nat. Chem. Biol.*, 2005, **1**, 13–21.
- 17 E. Saxon and C. R. Bertozzi, *Science*, 2000, **287**, 2007–2010.
- 18 S. Ghosh and S. Roseman, *J. Biol. Chem.*, 1965, **240**, 1531–1536.
- 19 S. J. Luchansky, K. J. Yarema, S. Takahashi and C. R. Bertozzi, *J. Biol. Chem.*, 2003, **278**, 8035–8042.
- 20 M. Boyce, I. S. Carrico, A. S. Ganguli, S.-H. Yu, M. J. Hangauer, S. C. Hubbard, J. J. Kohler and C. R. Bertozzi, *Proc. Natl. Acad. Sci. U. S. A.*, 2011, **108**, 3141–3146.
- 21 C. T. Saeui, E. Urias, L. Liu, M. P. Mathew and K. J. Yarema, *Glycoconjugate J.*, 2015, **32**, 425–441.
- 22 P. Luong and D. H. Dube, *Bioorg. Med. Chem.*, 2021, **42**, 116268.
- 23 N. Banahene, H. W. Kavunja and B. M. Swarts, *Chem. Rev.*, 2022, **122**, 3336–3413.

- 24 E. M. Sletten and C. R. Bertozzi, *Angew. Chem., Int. Ed.*, 2009, **48**, 6974–6998.
- 25 E. M. Sletten and C. R. Bertozzi, *Acc. Chem. Res.*, 2011, **44**, 666–676.
- 26 H. C. Hang, C. Yu, D. L. Kato and C. R. Bertozzi, *Proc. Natl. Acad. Sci. U. S. A.*, 2003, **100**, 14846–14851.
- 27 <https://www.nobelprize.org>.
- 28 V. Rigolot, C. Biot and C. Lion, *Angew. Chem., Int. Ed.*, 2021, **60**, 23084–23105.
- 29 T. Deb, J. Tu and R. M. Franzini, *Chem. Rev.*, 2021, **121**, 6850–6914.
- 30 G. S. Kumar and Q. Lin, *Chem. Rev.*, 2021, **121**, 6991–7031.
- 31 L. M. Haiber, M. Kufleitner and V. Wittmann, *Front. Chem.*, 2021, **9**, 654932.
- 32 S. S. Nguyen and J. A. Prescher, *Nat. Rev. Chem.*, 2020, **4**, 476–489.
- 33 B. L. Oliveira, Z. Guo and G. J. L. Bernardes, *Chem. Soc. Rev.*, 2017, **46**, 4895–4950.
- 34 S. L. Scinto, D. A. Bilodeau, R. Hincapie, W. Lee, S. S. Nguyen, M. Xu, C. W. am Ende, M. G. Finn, K. Lang, Q. Lin, J. P. Pezacki, J. A. Prescher, M. S. Robillard and J. M. Fox, *Nat. Rev. Methods Primers*, 2021, **1**, 30.
- 35 J. Shao and J. P. Tam, *J. Am. Chem. Soc.*, 1995, **117**, 3893–4200.
- 36 E. Saxon, S. J. Luchansky, H. C. Hang, C. Yu, S. C. Lee and C. R. Bertozzi, *J. Am. Chem. Soc.*, 2002, **124**, 14893–14902.
- 37 P. Crisalli and E. T. Kool, *J. Org. Chem.*, 2013, **78**, 1184–1189.
- 38 D. K. Kölmel and E. T. Kool, *Chem. Rev.*, 2017, **117**, 10358–10376.
- 39 H. Staudinger and J. Meyer, *Helv. Chim. Acta*, 1919, **2**, 635–646.
- 40 F. L. Lin, H. M. Hoyt, H. Van Halbeek, R. G. Bergman and C. R. Bertozzi, *J. Am. Chem. Soc.*, 2005, **127**, 2686–2695.
- 41 S. Bräse, C. Gil, K. Knepper and V. Zimmermann, *Angew. Chem., Int. Ed.*, 2005, **44**, 5188–5240.
- 42 J. A. Prescher, D. H. Dube and C. R. Bertozzi, *Nature*, 2004, **430**, 873–877.
- 43 E. Saxon, J. I. Armstrong and C. R. Bertozzi, *Org. Lett.*, 2000, **2**, 2141–2143.
- 44 B. L. Nilsson, L. L. Kiessling and R. T. Raines, *Org. Lett.*, 2000, **2**, 1939–1941.
- 45 X. Zhu, J. Liu and W. Zhang, *Nat. Chem. Biol.*, 2015, **11**, 115–120.
- 46 J. A. Marchand, M. E. Neugebauer, M. C. Ing, C. I. Lin, J. G. Pelton and M. C. Y. Chang, *Nature*, 2019, **567**, 420–424.
- 47 R. Huisgen, *Angew. Chem., Int. Ed. Engl.*, 1963, **2**, 565–598.
- 48 M. Breugst and H.-U. Reissig, *Angew. Chem., Int. Ed.*, 2020, **59**, 12293–12307.
- 49 C. W. Tornøe, C. Christensen and M. Meldal, *J. Org. Chem.*, 2002, **67**, 3057–3064.
- 50 V. V. Rostovtsev, L. G. Green, V. V. Fokin and K. B. Sharpless, *Angew. Chem., Int. Ed.*, 2002, **41**, 2596–2599.
- 51 B. T. Worrell, J. A. Malik and V. V. Fokin, *Science*, 2013, **340**, 457–460.
- 52 V. Hong, S. I. Presolski, C. Ma and M. G. Finn, *Angew. Chem., Int. Ed.*, 2009, **48**, 9879–9883.
- 53 S. I. Presolski, V. P. Hong and M. G. Finn, *Curr. Protoc. Chem. Biol.*, 2011, **3**, 153–162.
- 54 D. C. Kennedy, C. S. McKay, M. C. B. Legault, D. C. Danielson, J. A. Blake, A. F. Pegoraro, A. Stolor, Z. Mester and J. P. Pezacki, *J. Am. Chem. Soc.*, 2011, **133**, 17993–18001.
- 55 V. Hong, N. F. Steinmetz, M. Manchester and M. G. Finn, *Bioconjugate Chem.*, 2010, **21**, 1912–1916.
- 56 M. Meldal and C. W. Tornøe, *Chem. Rev.*, 2008, **108**, 2952–3015.
- 57 L. Liang and D. Astruc, *Coord. Chem. Rev.*, 2011, **255**, 2933–2945.
- 58 G. Wittig and A. Krebs, *Chem. Ber.*, 1961, **94**, 3260–3275.
- 59 N. J. Agard, J. A. Prescher and C. R. Bertozzi, *J. Am. Chem. Soc.*, 2004, **126**, 15046–15047.
- 60 D. H. Ess, G. O. Jones and K. N. Houk, *Org. Lett.*, 2008, **10**, 1633–1636.
- 61 N. J. Agard, J. M. Baskin, J. A. Prescher, A. Lo and C. R. Bertozzi, *ACS Chem. Biol.*, 2006, **1**, 644–648.
- 62 J. M. Baskin, J. A. Prescher, S. T. Laughlin, N. J. Agard, P. V. Chang, I. A. Miller, A. Lo, J. A. Codelli and C. R. Bertozzi, *Proc. Natl. Acad. Sci. U. S. A.*, 2007, **104**, 16793–16797.
- 63 J. A. Codelli, J. M. Baskin, N. J. Agard and C. R. Bertozzi, *J. Am. Chem. Soc.*, 2008, **130**, 11486–11493.
- 64 X. Ning, J. Guo, M. A. Wolfert and G.-J. Boons, *Angew. Chem., Int. Ed.*, 2008, **47**, 2253–2255.
- 65 B. Gold, G. B. Dudley and I. V. Alabugin, *J. Am. Chem. Soc.*, 2013, **135**, 1558–1569.
- 66 J. Dommerholt, F. P. J. T. Rutjes and F. L. van Delft, *Top. Curr. Chem.*, 2016, **374**, 16.
- 67 R. van Geel, G. J. M. Pruijn, F. L. van Delft and W. C. Boelens, *Bioconjugate Chem.*, 2012, **23**, 392–398.
- 68 R. A. Carboni and R. V. Lindsey, *J. Am. Chem. Soc.*, 1959, **81**, 4342–4346.
- 69 M. L. Blackman, M. Royzen and J. M. Fox, *J. Am. Chem. Soc.*, 2008, **130**, 13518–13519.
- 70 N. K. Devaraj, R. Weissleder and S. A. Hilderbrand, *Bioconjugate Chem.*, 2008, **19**, 2297–2299.
- 71 K. Braun, M. Wiessler, V. Ehemann, R. Pipkorn, H. Spring, J. Debus, B. Diding, M. Koch, G. Muller and W. Waldeck, *Drug Des., Dev. Ther.*, 2008, **2**, 289–301.
- 72 D. M. Patterson, L. A. Nazarova, B. Xie, D. N. Kamber and J. A. Prescher, *J. Am. Chem. Soc.*, 2012, **134**, 18638–18643.
- 73 D.-C. Xiong, J. Zhu, M.-J. Han, H.-X. Luo, C. Wang, Y. Yu, Y. Ye, G. Tai and X.-S. Ye, *Org. Biomol. Chem.*, 2015, **13**, 3911–3917.
- 74 J. Hassenrück and V. Wittmann, *Beilstein J. Org. Chem.*, 2019, **15**, 584–601.
- 75 J. Yang, J. Šečutė, C. M. Cole and N. K. Devaraj, *Angew. Chem., Int. Ed.*, 2012, **51**, 7476–7479.
- 76 A.-K. Späte, J. E. G. A. Dold, E. Batroff, V. F. Schart, D. E. Wieland, O. R. Baudendistel and V. Wittmann, *ChemBioChem*, 2016, **17**, 1374–1383.

- 77 R. Zhang, J. Zheng and T. Zhang, *RSC Adv.*, 2020, **10**, 15990–15996.
- 78 F. Doll, A. Buntz, A.-K. Späte, V. F. Schart, A. Timper, W. Schrimpf, C. R. Hauck, A. Zumbusch and V. Wittmann, *Angew. Chem., Int. Ed.*, 2016, **55**, 2262–2266.
- 79 H. Stöckmann, A. A. Neves, S. Stairs, K. M. Brindle and F. J. Leeper, *Org. Biomol. Chem.*, 2011, **9**, 7303–7305.
- 80 S. Stairs, A. A. Neves, H. Stöckmann, Y. A. Wainman, H. Ireland-Zecchini, K. M. Brindle and F. J. Leeper, *ChemBioChem*, 2013, **14**, 1063–1067.
- 81 J. Tu, M. Xu, S. Parvez, R. T. Peterson and R. M. Franzini, *J. Am. Chem. Soc.*, 2018, **140**, 8410–8414.
- 82 R. J. B. Schäfer, M. R. Monaco, M. Li, A. Tirla, P. Rivera-Fuentes and H. Wennemers, *J. Am. Chem. Soc.*, 2019, **141**, 18644–18648.
- 83 R. Huisgen, R. Grashey, H. Gotthardt and R. Schmidt, *Angew. Chem., Int. Ed. Engl.*, 1962, **1**, 48–49.
- 84 S. Kolodych, E. Rasolofonjatovo, M. Chaumontet, M.-C. Nevers, C. Créminon and F. Taran, *Angew. Chem., Int. Ed.*, 2013, **52**, 12056–12060.
- 85 S. Wallace and J. W. Chin, *Chem. Sci.*, 2014, **5**, 1742–1744.
- 86 L. Plougastel, O. Koniev, S. Specklin, E. Decuypere, C. Créminon, D.-A. Buisson, A. Wagner, S. Kolodych and F. Taran, *Chem. Commun.*, 2014, **50**, 9376–9378.
- 87 T. R. Gimadiev, O. Klimchuk, R. I. Nugmanov, T. I. Madzhidov and A. Varnek, *J. Mol. Struct.*, 2019, **1198**, 126897.
- 88 E. Decuypère, M. Riomet, A. Sallustrau, S. Bregant, R. Thai, G. Pieters, G. Clavier, D. Audisio and F. Taran, *Chem. Commun.*, 2018, **54**, 10758–10761.
- 89 L. Plougastel, M. R. Pattanayak, M. Riomet, S. Bregant, A. Sallustrau, M. Nothisen, A. Wagner, D. Audisio and F. Taran, *Chem. Commun.*, 2019, **55**, 4582–4585.
- 90 Z. S. Chinoy, C. Bodineau, C. Favre, K. W. Moremen, R. V. Durán and F. Friscourt, *Angew. Chem., Int. Ed.*, 2019, **58**, 4281–4285.
- 91 K. Krell, B. Pfeuffer, F. Rönicke, Z. S. Chinoy, C. Favre, F. Friscourt and H.-A. Wagenknecht, *Chem. – Eur. J.*, 2021, **27**, 16093–16097.
- 92 Y. Wang, C. I. Rivera Vera and Q. Lin, *Org. Lett.*, 2007, **9**, 4155–4158.
- 93 J. S. Clovis, A. Eckell, R. Huisgen and R. Sustmann, *Chem. Ber.*, 1967, **100**, 60–70.
- 94 R. K. V. Lim and Q. Lin, *Acc. Chem. Res.*, 2011, **44**, 828–839.
- 95 Z. Yu, Y. Pan, Z. Wang, J. Wang and Q. Lin, *Angew. Chem., Int. Ed.*, 2012, **51**, 10600–10604.
- 96 Y. Wang, W. J. Hu, W. Song, R. K. V. Lim and Q. Lin, *Org. Lett.*, 2008, **10**, 3725–3728.
- 97 Y. Wang and Q. Lin, *Org. Lett.*, 2009, **11**, 3570–3573.
- 98 Z. Yu, L. Y. Ho and Q. Lin, *J. Am. Chem. Soc.*, 2011, **133**, 11912–11915.
- 99 V. F. Schart, J. Hassenrück, A.-K. Späte, J. E. G. A. Dold, R. Fahrner and V. Wittmann, *ChemBioChem*, 2019, **20**, 166–171.
- 100 K. Krell, D. Harijan, D. Ganz, L. Doll and H.-A. Wagenknecht, *Bioconjugate Chem.*, 2020, **31**, 990–1011.
- 101 G. Delaittre, A. S. Goldmann, J. O. Mueller and C. Barner-Kowollik, *Angew. Chem., Int. Ed.*, 2015, **54**, 11388–11403.
- 102 E. Blasco, M. Wegener and C. Barner-Kowollik, *Adv. Mater.*, 2017, **29**, 1604005.
- 103 M. Sawa, T.-L. Hsu, T. Itoh, M. Sugiyama, S. R. Hanson, P. K. Vogt and C.-H. Wong, *Proc. Natl. Acad. Sci. U. S. A.*, 2006, **103**, 12371–12376.
- 104 P. V. Chang, J. A. Prescher, M. J. Hangauer and C. R. Bertozzi, *J. Am. Chem. Soc.*, 2007, **129**, 8400–8401.
- 105 T.-L. Hsu, S. R. Hanson, K. Kishikawa, S.-K. Wang, M. Sawa and C.-H. Wong, *Proc. Natl. Acad. Sci. U. S. A.*, 2007, **104**, 2614–2619.
- 106 Y. Kizuka, S. Funayama, H. Shogomori, M. Nakano, K. Nakajima, R. Oka, S. Kitazume, Y. Yamaguchi, M. Sano, H. Korekane, T.-L. Hsu, H.-Y. Lee, C.-H. Wong and N. Taniguchi, *Cell Chem. Biol.*, 2016, **23**, 782–792.
- 107 Y. Haga, K. Ishii, K. Hibino, Y. Sako, Y. Ito, N. Taniguchi and T. Suzuki, *Nat. Commun.*, 2012, **3**, 907.
- 108 B. Belardi, A. de la Zerda, D. R. Spiciarich, S. L. Maund, D. M. Peehl and C. R. Bertozzi, *Angew. Chem., Int. Ed.*, 2013, **52**, 14045–14049.
- 109 L. Zhu, Y. Xu, X. Wei, H. Lin, M. Huang, B. Lin, Y. Song and C. Yang, *Angew. Chem., Int. Ed.*, 2021, **60**, 18111–18115.
- 110 W. Lin, Y. Du, Y. Zhu and X. Chen, *J. Am. Chem. Soc.*, 2014, **136**, 679–687.
- 111 N. Wu, L. Bao, L. Ding and H. Ju, *Angew. Chem., Int. Ed.*, 2016, **55**, 5220–5224.
- 112 N. Li, W. Zhang, L. Lin, S. N. A. Shah, Y. Li and J.-M. Lin, *Anal. Chem.*, 2019, **91**, 2600–2604.
- 113 X. Zhang, R. Li, Y. Chen, S. Zhang, W. Wang and F. Li, *Chem. Sci.*, 2016, **7**, 6182–6189.
- 114 X. Wen, B. Yuan, J. Zhang, X. Meng, Q. Guo, L. Li, Z. Li, H. Jiang and K. Wang, *Chem. Commun.*, 2019, **55**, 6114–6117.
- 115 J. Li, S. Liu, L. Sun, W. Li, S.-Y. Zhang, S. Yang, J. Li and H.-H. Yang, *J. Am. Chem. Soc.*, 2018, **140**, 16589–16595.
- 116 B. Yuan, Y. Chen, Y. Sun, Q. Guo, J. Huang, J. Liu, X. Meng, X. Yang, X. Wen, Z. Li, L. Li and K. Wang, *Anal. Chem.*, 2018, **90**, 6131–6137.
- 117 A. Niederwieser, A.-K. Späte, L. D. Nguyen, C. Jüngst, W. Reutter and V. Wittmann, *Angew. Chem., Int. Ed.*, 2013, **52**, 4265–4268.
- 118 A.-K. Späte, V. F. Schart, S. Schöllkopf, A. Niederwieser and V. Wittmann, *Chem. – Eur. J.*, 2014, **20**, 16502–16508.
- 119 J. E. G. A. Dold, J. Pfozter, A.-K. Späte and V. Wittmann, *ChemBioChem*, 2017, **18**, 1242–1250.
- 120 J. E. G. A. Dold and V. Wittmann, *ChemBioChem*, 2021, **22**, 1243–1251.
- 121 A. Kitowski and G. J. L. Bernardes, *ChemBioChem*, 2020, **21**, 2696–2700.
- 122 C. M. Cole, J. Yang, J. Ščkutě and N. K. Devaraj, *ChemBioChem*, 2013, **14**, 205–208.
- 123 A.-K. Späte, H. Bußkamp, A. Niederwieser, V. F. Schart, A. Marx and V. Wittmann, *Bioconjugate Chem.*, 2014, **25**, 147–154.
- 124 D. M. Patterson, K. A. Jones and J. A. Prescher, *Mol. Biosyst.*, 2014, **10**, 1693–1697.

- 125 A.-K. Späte, V. F. Schart, J. Häfner, A. Niederwieser, T. U. Mayer and V. Wittmann, *Beilstein J. Org. Chem.*, 2014, **10**, 2235–2242.
- 126 P. Agarwal, B. J. Beahm, P. Shieh and C. R. Bertozzi, *Angew. Chem., Int. Ed.*, 2015, **54**, 11504–11510.
- 127 Y. A. Wainman, A. A. Neves, S. Stairs, H. Stöckmann, H. Ireland-Zecchini, K. M. Brindle and F. J. Leeper, *Org. Biomol. Chem.*, 2013, **11**, 7297–7300.
- 128 D. Benito-Alifonso, S. Tremell, J. C. Sadler, M. Berry and M. C. Galan, *Chem. Commun.*, 2016, **52**, 4906–4909.
- 129 Y. Tanaka and J. J. Kohler, *J. Am. Chem. Soc.*, 2008, **130**, 3278–3279.
- 130 M. R. Bond, H. Zhang, J. Kim, S.-H. Yu, F. Yang, S. M. Patrie and J. J. Kohler, *Bioconjugate Chem.*, 2011, **22**, 1811–1823.
- 131 M. R. Bond, C. M. Whitman and J. J. Kohler, *Mol. Biosyst.*, 2010, **6**, 1796–1799.
- 132 H. Wu, A. Shajahan, J.-Y. Yang, E. Capota, A. M. Wands, C. M. Arthur, S. R. Stowell, K. W. Moremen, P. Azadi and J. J. Kohler, *Cell Chem. Biol.*, 2022, **29**, 84–97.
- 133 E. Zhang, Y. Shi, J. Han and S. Han, *Anal. Chem.*, 2020, **92**, 15059–15068.
- 134 P. Kranaster, C. Karreman, J. E. G. A. Dold, A. Krebs, M. Funke, A.-K. Holzer, S. Klima, J. Nyffeler, S. Helfrich, V. Wittmann and M. Leist, *Arch. Toxicol.*, 2020, **94**, 449–467.
- 135 R. A. Flynn, K. Pedram, S. A. Malaker, P. J. Batista, B. A. H. Smith, A. G. Johnson, B. M. George, K. Majzoub, P. W. Villalta, J. E. Carette and C. R. Bertozzi, *Cell*, 2021, **184**, 3109–3124.
- 136 R. M. F. Tomás, B. Martyn, T. L. Bailey and M. I. Gibson, *ACS Macro Lett.*, 2018, **7**, 1289–1294.
- 137 R. M. F. Tomás and M. I. Gibson, *Biomacromolecules*, 2019, **20**, 2726–2736.
- 138 M. Ghirardello, R. Shyam and M. C. Galan, *Chem. Commun.*, 2022, **58**, 5522–5525.
- 139 C.-R. Torres and G. W. Hart, *J. Biol. Chem.*, 1984, **259**, 3308–3317.
- 140 G. D. Holt and G. W. Hart, *J. Biol. Chem.*, 1986, **261**, 8049–8057.
- 141 J. Ma, C. Wu and G. W. Hart, *Chem. Rev.*, 2021, **121**, 1513–1581.
- 142 B. W. Zaro, Y.-Y. Yang, H. C. Hang and M. R. Pratt, *Proc. Natl. Acad. Sci. U. S. A.*, 2011, **108**, 8146–8151.
- 143 J. Li, J. Wang, L. Wen, H. Zhu, S. Li, K. Huang, K. Jiang, X. Li, C. Ma, J. Qu, A. Parameswaran, J. Song, W. Zhao and P. G. Wang, *ACS Chem. Biol.*, 2016, **11**, 3002–3006.
- 144 K. N. Chuh, B. W. Zaro, F. Piller, V. Piller and M. R. Pratt, *J. Am. Chem. Soc.*, 2014, **136**, 12283–12295.
- 145 W. Qin, P. Lv, X. Fan, B. Quan, Y. Zhu, K. Qin, Y. Chen, C. Wang and X. Chen, *Proc. Natl. Acad. Sci. U. S. A.*, 2017, **114**, E6749–E6758.
- 146 T. W. Liu, M. Myschyshyn, D. A. Sinclair and D. J. Vocadlo, *ACS Cent. Sci.*, 2019, **5**, 663–670.
- 147 C. M. Woo, P. J. Lund, A. C. Huang, M. M. Davis, C. R. Bertozzi and S. J. Pitteri, *Mol. Cell. Proteomics*, 2018, **17**, 764–775.
- 148 D. L. Shen, T.-W. Liu, W. Zandberg, T. Clark, R. Eskandari, M. G. Alteen, H. Y. Tan, Y. Zhu, S. Cecioni and D. Vocadlo, *ACS Chem. Biol.*, 2017, **12**, 206–213.
- 149 B. W. Zaro, A. R. Batt, K. N. Chuh, M. X. Navarro and M. R. Pratt, *ACS Chem. Biol.*, 2017, **12**, 787–794.
- 150 J. Guo, G. Zhang, J. Ma, C. Zhao, Q. Xue, J. Wang, W. Liu, K. Liu, H. Wang, N. Liu, Q. Song and J. Li, *Org. Biomol. Chem.*, 2019, **17**, 4326–4334.
- 151 E. G. Jackson, G. Cutolo, B. Yang, N. Yarravarapu, M. W. N. Burns, G. Bineva-Todd, C. Roustan, J. B. Thoden, H. M. Lin-Jones, T. H. van Kuppevelt, H. M. Holden, B. Schumann, J. J. Kohler, C. M. Woo and M. R. Pratt, *ACS Chem. Biol.*, 2022, **17**, 159–170.
- 152 H. Y. Tan, R. Eskandari, D. Shen, Y. Zhu, T.-W. Liu, L. I. Willems, M. G. Alteen, Z. Madden and D. J. Vocadlo, *J. Am. Chem. Soc.*, 2018, **140**, 15300–15308.
- 153 C. A. Kondor, J. N. Gorantla, G. D. Leonard and C. Fehl, *Bioorg. Med. Chem.*, 2022, **70**, 116918.
- 154 Y. Zhu, T.-W. Liu, S. Cecioni, R. Eskandari, W. F. Zandberg and D. J. Vocadlo, *Nat. Chem. Biol.*, 2015, **11**, 319–325.
- 155 Y. Zhu, L. I. Willems, D. Salas, S. Cecioni, W. B. Wu, L. J. Foster and D. J. Vocadlo, *J. Am. Chem. Soc.*, 2020, **142**, 15729–15739.
- 156 W. Lin, L. Gao and X. Chen, *ChemBioChem*, 2015, **16**, 2571–2575.
- 157 A. Kasprowicz, C. Spriet, C. Terryn, V. Rigolot, S. Hardiville, M. G. Alteen, T. Lefebvre and C. Biot, *Molecules*, 2020, **25**, 4501.
- 158 W. Qin, K. Qin, X. Fan, L. Peng, W. Hong, Y. Zhu, P. Lv, Y. Du, R. Huang, M. Han, B. Cheng, Y. Liu, W. Zhou, C. Wang and X. Chen, *Angew. Chem., Int. Ed.*, 2018, **57**, 1817–1820.
- 159 N. Darabedian, B. Yang, R. Ding, G. Cutolo, B. W. Zaro, C. M. Woo and M. R. Pratt, *Front. Chem.*, 2020, **8**, 00318.
- 160 K. Qin, H. Zhang, Z. Zhao and X. Chen, *J. Am. Chem. Soc.*, 2020, **142**, 9382–9388.
- 161 Y. Hao, X. Fan, Y. Shi, C. Zhang, D.-E. Sun, K. Qin, W. Qin, W. Zhou and X. Chen, *Nat. Commun.*, 2019, **10**, 4065.
- 162 X. Fan, Q. Song, D.-E. Sun, Y. Hao, J. Wang, C. Wang and X. Chen, *Nat. Chem. Biol.*, 2022, **18**, 625–633.
- 163 N. J. Pedowitz, E. G. Jackson, J. M. Overhulse, C. E. McKenna, J. J. Kohler and M. R. Pratt, *ACS Chem. Biol.*, 2021, **16**, 1924–1929.
- 164 S.-H. Yu, M. Boyce, A. M. Wands, M. R. Bond, C. R. Bertozzi and J. J. Kohler, *Proc. Natl. Acad. Sci. U. S. A.*, 2012, **109**, 4834–4839.
- 165 A. C. Rodriguez and J. J. Kohler, *MedChemComm*, 2014, **5**, 1227–1234.
- 166 B. N. Kakde, E. Capota, J. J. Kohler and U. K. Tambar, *J. Org. Chem.*, 2021, **86**, 18257–18264.
- 167 J. Choi, L. J. S. Wagner, S. B. P. E. Timmermans, S. A. Malaker, B. Schumann, M. A. Gray, M. F. Debets, M. Takashima, J. Gehring and C. R. Bertozzi, *J. Am. Chem. Soc.*, 2019, **141**, 13442–13453.
- 168 B. Schumann, S. A. Malaker, S. P. Wisnovsky, M. F. Debets, A. J. Agbay, D. Fernandez, L. J. S. Wagner, L. Lin, Z. Li,

- J. Choi, D. M. Fox, J. Peh, M. A. Gray, K. Pedram, J. J. Kohler, M. Mrksich and C. R. Bertozzi, *Mol. Cell*, 2020, **78**, 824–834.
- 169 F. Debets Marjoke, Y. Tastan Omur, P. Wisnovsky Simon, A. Malaker Stacy, N. Angelis, K. R. Moeckl Leonhard, J. Choi, H. Flynn, J. S. Wagner Lauren, G. Bineva-Todd, A. Antonopoulos, A. Cioce, M. Browne William, Z. Li, C. Briggs David, L. Douglas Holly, T. Hess Gaelen, J. Agbay Anthony, C. Roustan, S. Kjaer, M. Haslam Stuart, P. Snijders Ambrosius, C. Bassik Michael, W. E. Moerner, S. W. Li Vivian, R. Bertozzi Carolyn and B. Schumann, *Proc. Natl. Acad. Sci. U. S. A.*, 2020, **117**, 25293–25301.
- 170 A. Cioce, G. Bineva-Todd, A. J. Agbay, J. Choi, T. M. Wood, M. F. Debets, W. M. Browne, H. L. Douglas, C. Roustan, O. Y. Tastan, S. Kjaer, J. T. Bush, C. R. Bertozzi and B. Schumann, *ACS Chem. Biol.*, 2021, **16**, 1961–1967.
- 171 B. Calle, G. Bineva-Todd, A. Marchesi, H. Flynn, M. Ghirardello, O. Y. Tastan, C. Roustan, J. Choi, M. C. Galan, B. Schumann and S. A. Malaker, *J. Am. Soc. Mass Spectrom.*, 2021, **32**, 2366–2375.
- 172 C. Frantz, K. M. Stewart and V. M. Weaver, *J. Cell Sci.*, 2010, **123**, 4195–4200.
- 173 P. S. Briquez, J. A. Hubbell and M. M. Martino, *Adv. Wound Care*, 2015, **4**, 479–489.
- 174 J. Zhu and R. A. F. Clark, *J. Invest. Dermatol.*, 2014, **134**, 895–901.
- 175 M. W. Tibbitt and K. S. Anseth, *Biotechnol. Bioeng.*, 2009, **103**, 655–663.
- 176 L. E. Fitzpatrick and T. C. McDevitt, *Biomater. Sci.*, 2015, **3**, 12–24.
- 177 S. M. Ruff, S. Keller, D. E. Wieland, V. Wittmann, G. E. M. Tovar, M. Bach and P. J. Kluger, *Acta Biomater.*, 2017, **52**, 159–170.
- 178 S. Nellinger, S. Keller, A. Southan, V. Wittmann, A.-C. Volz and P. J. Kluger, *Curr. Dir. Biomed. Eng.*, 2019, **5**, 393–395.
- 179 M. Gutmann, A. Braun, J. Seibel and T. Lühmann, *ACS Biomater. Sci. Eng.*, 2018, **4**, 1300–1306.
- 180 M. Gutmann, J. Bechold, J. Seibel, L. Meinel and T. Lühmann, *ACS Biomater. Sci. Eng.*, 2019, **5**, 215–233.
- 181 S. Nellinger, M. A. Rapp, A. Southan, V. Wittmann and P. J. Kluger, *ChemBioChem*, 2022, **23**, e202100266.
- 182 S. S. Pinho and C. A. Reis, *Nat. Rev. Cancer*, 2015, **15**, 540–555.
- 183 K. F. Boligan, C. Mesa, L. E. Fernandez and S. von Gunten, *Cell. Mol. Life Sci.*, 2015, **72**, 1231–1248.
- 184 A. A. Neves, Y. A. Wainman, A. Wright, M. I. Kettunen, T. B. Rodrigues, S. McGuire, D.-E. Hu, F. Bulat, S. Geninatti Crich, H. Stöckmann, F. J. Leeper and K. M. Brindle, *Angew. Chem., Int. Ed.*, 2016, **55**, 1286–1290.
- 185 Y. Zhao, S. Li, J. Lv, Y. Liu, Y. Chen, Y. Liu, X. Chen, J. Li, X. Qin, X. Wang, J. Shi, Y. Shi and R. Xiang, *Theranostics*, 2021, **11**, 7425–7438.
- 186 Z. Zhao, Z. Zhang, S. Duan, X. Liu, R. Zhou, M. Hou, Y. Sang, R. Zhu and L. Yin, *Biomater. Sci.*, 2021, **9**, 4639–4647.
- 187 J. Liu, F. Hu, M. Wu, L. Tian, F. Gong, X. Zhong, M. Chen, Z. Liu and B. Liu, *Adv. Mater.*, 2021, **33**, 2007888.
- 188 L. Qiu, J. Li, S. Yu, Q. Wang, Y. Li, Z. Hu, Q. Wu, Z. Guo and J. Zhang, *Oncotarget*, 2015, **6**, 5195–5203.
- 189 D. H. Dube and C. R. Bertozzi, *Nat. Rev. Drug Discovery*, 2005, **4**, 477–488.
- 190 M. Li, L. Song and X. Qin, *J. Biosci.*, 2010, **35**, 665–673.
- 191 L. Qiu, X. Gong, Q. Wang, J. Li, H. Hu, Q. Wu, J. Zhang and Z. Guo, *Cancer Immunol. Immunother.*, 2012, **61**, 2045–2054.
- 192 H. Wang, M. C. Sobral, D. K. Y. Zhang, A. N. Cartwright, A. W. Li, M. O. Dellacherie, C. M. Tringides, S. T. Koshy, K. W. Wucherpfennig and D. J. Mooney, *Nat. Mater.*, 2020, **19**, 1244–1252.
- 193 C. Büll, T. Heise, N. van Hilten, J. F. A. Pijnenborg, V. R. L. J. Bloemendal, L. Gerrits, E. D. Kers-Rebel, T. Ritschel, M. H. den Brok, G. J. Adema and T. J. Boltje, *Angew. Chem., Int. Ed.*, 2017, **56**, 3309–3313.
- 194 H. Maeda, *Adv. Drug Delivery Rev.*, 2015, **91**, 3–6.
- 195 H. H. Gustafson, D. Holt-Casper, D. W. Grainger and H. Ghandehari, *Nano Today*, 2015, **10**, 487–510.
- 196 H. Koo, S. Lee, J. H. Na, S. H. Kim, S. K. Hahn, K. Choi, I. C. Kwon, S. Y. Jeong and K. Kim, *Angew. Chem., Int. Ed.*, 2012, **51**, 11836–11840.
- 197 H. Y. Yoon, M. L. Shin, M. K. Shim, S. Lee, J. H. Na, H. Koo, H. Lee, J. H. Kim, K. Y. Lee, K. Kim and I. C. Kwon, *Mol. Pharmaceutics*, 2017, **14**, 1558–1570.
- 198 L. Du, H. Qin, T. Ma, T. Zhang and D. Xing, *ACS Nano*, 2017, **11**, 8930–8943.
- 199 S. Lee, S. Jung, H. Koo, J. H. Na, H. Y. Yoon, M. K. Shim, J. Park, J.-H. Kim, S. Lee, M. G. Pomper, I. C. Kwon, C.-H. Ahn and K. Kim, *Biomaterials*, 2017, **148**, 1–15.
- 200 R. Xie, S. Hong, L. Feng, J. Rong and X. Chen, *J. Am. Chem. Soc.*, 2012, **134**, 9914–9917.
- 201 S. Lee, H. Koo, J. H. Na, S. J. Han, H. S. Min, S. J. Lee, S. H. Kim, S. H. Yun, S. Y. Jeong, I. C. Kwon, K. Choi and K. Kim, *ACS Nano*, 2014, **8**, 2048–2063.
- 202 S. Lim, H. Y. Yoon, H. J. Jang, S. Song, W. Kim, J. Park, K. E. Lee, S. Jeon, S. Lee, D.-K. Lim, B.-S. Kim, D.-E. Kim and K. Kim, *ACS Nano*, 2019, **13**, 10991–11007.
- 203 Y. Zhai, J. Su, W. Ran, P. Zhang, Q. Yin, Z. Zhang, H. Yu and Y. Li, *Theranostics*, 2017, **7**, 2575–2592.
- 204 P. G. Coulie, B. J. Van den Eynde, P. van der Bruggen and T. Boon, *Nat. Rev. Cancer*, 2014, **14**, 135–146.
- 205 Y. Han, H. Pan, W. Li, Z. Chen, A. Ma, T. Yin, R. Liang, F. Chen, Y. Ma, Y. Jin, M. Zheng, B. Li and L. Cai, *Adv. Sci.*, 2019, **6**, 1900251.
- 206 M. Tkach and C. Théry, *Cell*, 2016, **164**, 1226–1232.
- 207 G. T. Lim, D. G. You, H. S. Han, H. Lee, S. Shin, B. H. Oh, E. K. P. Kumar, W. Um, C. H. Kim, S. Han, S. Lee, S. Lim, H. Y. Yoon, K. Kim, I. C. Kwon, D.-G. Jo, Y. W. Cho and J. H. Park, *J. Extracell. Vesicles*, 2021, **10**, e12077.
- 208 S. Y. Gun, S. W. L. Lee, J. L. Sieow and S. C. Wong, *Redox. Biol.*, 2019, **25**, 101174.
- 209 X. Wang, S. Lang, Y. Tian, J. Zhang, X. Yan, Z. Fang, J. Weng, N. Lu, X. Wu, T. Li, H. Cao, Z. Li and X. Huang, *ACS Cent. Sci.*, 2020, **6**, 382–389.
- 210 C. D. Rillahan, M. S. Macauley, E. Schwartz, Y. He, R. McBride, B. M. Arlian, J. Rangarajan, V. V. Fokin and J. C. Paulson, *Chem. Sci.*, 2014, **5**, 2398–2406.

- 211 X. Wang, X. Luo, Y. Tian, T. Wu, J. Weng, Z. Li, F. Ye and X. Huang, *ACS Chem. Biol.*, 2021, **16**, 724–730.
- 212 S. A. Rosenberg and N. P. Restifo, *Science*, 2015, **348**, 62–68.
- 213 J. Corrigan-Curay, H. P. Kiem, D. Baltimore, M. O'Reilly, R. J. Brentjens, L. Cooper, S. Forman, S. Gottschalk, P. Greenberg, R. Junghans, H. Heslop, M. Jensen, C. Mackall, C. June, O. Press, D. Powell, A. Ribas, S. Rosenberg, M. Sadelain, B. Till, A. P. Patterson, R. C. Jambou, E. Rosenthal, L. Gargiulo, M. Montgomery and D. B. Kohn, *Mol. Ther.*, 2014, **22**, 1564–1574.
- 214 H. Pan, P. Li, G. Li, W. Li, B. Hu, H. He, Z. Chen, F. Wang, L. Liu, Y. Gong, Y. Han, Y. Luo, M. Zheng, Y. Ma, L. Cai and Y. Jin, *Adv. Funct. Mater.*, 2019, **29**, 1807528.
- 215 P. V. Chang, D. H. Dube, E. M. Sletten and C. R. Bertozzi, *J. Am. Chem. Soc.*, 2010, **132**, 9516–9518.
- 216 M. K. Shim, H. Y. Yoon, J. H. Ryu, H. Koo, S. Lee, J. H. Park, J.-H. Kim, S. Lee, M. G. Pomper, I. C. Kwon and K. Kim, *Angew. Chem., Int. Ed.*, 2016, **55**, 14698–14703.
- 217 H. Wang, R. Wang, K. Cai, H. He, Y. Liu, J. Yen, Z. Wang, M. Xu, Y. Sun, X. Zhou, Q. Yin, L. Tang, I. T. Dobrucki, L. W. Dobrucki, E. J. Chaney, S. A. Boppart, T. M. Fan, S. Lezmi, X. Chen, L. Yin and J. Cheng, *Nat. Chem. Biol.*, 2017, **13**, 415–424.
- 218 Y. Li, L. Gong, H. Hong, H. Lin, D. Li, J. Shi, Z. Zhou and Z. Wu, *Chem. Commun.*, 2022, **58**, 2568–2571.
- 219 S.-W. Kang, S. Lee, J. H. Na, H. I. Yoon, D.-E. Lee, H. Koo, Y. W. Cho, S. H. Kim, S. Y. Jeong, I. C. Kwon, K. Choi and K. Kim, *Theranostics*, 2014, **4**, 420–431.
- 220 G. Chen, Y. Jin, X. Shi, Y. Qiu, Y. Zhang, M. Cheng, X. Wang, C. Chen, Y. Wu, F. Jiang, L. Li, H. Zhou, Q. Fu and X. Liu, *Stem Cell Res. Ther.*, 2015, **6**, 40.
- 221 N. Liao, D. Zhang, M. Wu, H. Yang, X. Liu and J. Song, *Nanoscale*, 2021, **13**, 1813–1822.
- 222 G. Chen, T. Ushida and T. Tateishi, *Macromol. Biosci.*, 2002, **2**, 67–77.
- 223 D. Mao, C. Zhang, Kenry, J. Liu, X. Wang, B. Li, H. Yan, F. Hu, D. Kong, Z. Wang and B. Liu, *Biomaterials*, 2020, **230**, 119615.
- 224 S. Altmann, J. Mut, N. Wolf, J. Meißner-Weigl, M. Rudert, F. Jakob, M. Gutmann, T. Lühmann, J. Seibel and R. Ebert, *Int. J. Mol. Sci.*, 2021, **22**, 2820.
- 225 K. M. Au, Y. Medik, Q. Ke, R. Tisch and A. Z. Wang, *Adv. Mater.*, 2021, **33**, 2101253.
- 226 S. T. Laughlin, J. M. Baskin, S. L. Amacher and C. R. Bertozzi, *Science*, 2008, **320**, 664–667.
- 227 J. M. Baskin, K. W. Dehnert, S. T. Laughlin, S. L. Amacher and C. R. Bertozzi, *Proc. Natl. Acad. Sci. U. S. A.*, 2010, **107**, 10360–10365.
- 228 K. W. Dehnert, B. J. Beahm, T. T. Huynh, J. M. Baskin, S. T. Laughlin, W. Wang, P. Wu, S. L. Amacher and C. R. Bertozzi, *ACS Chem. Biol.*, 2011, **6**, 547–552.
- 229 S. Hong, P. Sahai-Hernandez, D. G. Chapla, K. W. Moremen, D. Traver and P. Wu, *Angew. Chem., Int. Ed.*, 2019, **58**, 14327–14333.
- 230 J. L. Daughtry, W. Cao, J. Ye and J. M. Baskin, *ACS Chem. Biol.*, 2020, **15**, 318–324.
- 231 M. Ropitiaux, Q. Hays, A. Baron, L. Fourmois, I. Boulogne, B. Vauzeilles, P. Lerouge, J.-C. Mollet and A. Lehner, *Plant J.*, 2022, **110**, 916–924.
- 232 C. T. Anderson, I. S. Wallace and C. R. Somerville, *Proc. Natl. Acad. Sci. U. S. A.*, 2012, **109**, 1329–1334.
- 233 Y. Zhu and X. Chen, *ChemBioChem*, 2017, **18**, 1286–1296.
- 234 J. Hoogenboom, N. Berghuis, D. Cramer, R. Geurts, H. Zuillhof and T. Wennekes, *BMC Plant Biology*, 2016, **16**, 220.
- 235 C. Simon, C. Lion, C. Spriet, F. Baldacci-Cresp, S. Hawkins and C. Biot, *Angew. Chem., Int. Ed.*, 2018, **57**, 16665–16671.
- 236 M. Dumont, A. Lehner, B. Vauzeilles, J. Malassis, A. Marchant, K. Smyth, B. Linclau, A. Baron, J. Mas Pons, C. T. Anderson, D. Schapman, L. Galas, J.-C. Mollet and P. Lerouge, *Plant J.*, 2016, **85**, 437–447.
- 237 Y. Zhu, J. Wu and X. Chen, *Angew. Chem., Int. Ed.*, 2016, **55**, 9301–9305.